Nonequilibrium and local detection of the normal fraction of a trapped two-dimensional Bose gas

Iacopo Carusotto[1] and Yvan Castin[2]

[1]*INO-CNR BEC Center and Dipartimento di Fisica, Università di Trento, I-38123 Povo, Italy*

[2]*Laboratoire Kastler Brossel, École normale supérieure, UPMC and CNRS, 24 rue Lhomond, F-75231 Paris Cedex 05, France*

We propose a method to measure the normal fraction of a two-dimensional Bose gas, a quantity that generally differs from the noncondensed fraction. The idea is based on applying a spatially oscillating artificial gauge field to the atoms. The response of the atoms to the gauge field can be read out either mechanically from the deposited energy into the cloud or optically from the macroscopic optical properties of the atomic gas. The local nature of the proposed scheme allows one to reconstruct the spatial profile of the superfluid component; furthermore, the proposed method does not require having established thermal equilibrium in the gas in the presence of the gauge field. The theoretical description of the system is based on a generalization of the Dum-Olshanii theory of artificial gauge fields to the interacting many-body context. The efficiency of the proposed measurement scheme is assessed by means of classical field numerical simulations. An explicit atomic level scheme minimizing disturbing effects such as spontaneous emission and light shifts is proposed for ^{87}Rb atoms.

PACS number(s): 67.85.−d, 47.37.+q, 37.10.Vz, 42.50.Gy

I. INTRODUCTION

One of the most striking features of degenerate Bose gases in two dimensions is the possibility of having a superfluid behavior in the absence of a macroscopically populated Bose-Einstein condensate. The transition to the superfluid state is of the Berezinskii-Kosterlitz-Thouless (BKT) type, characterized by a sudden jump of the superfluid density from 0 to the universal value 4 (in units of the inverse square of the de Broglie thermal wavelength), independent from the details of the system [1,2]. At the transition point, the asymptotic behavior of the field correlation function changes from an exponential to a power-law decay at large distances. In contrast to the three-dimensional case, superfluidity is then not related to the appearance of a macroscopically occupied Bose-Einstein condensate in the thermodynamic limit.

Pioneering experiments have addressed the mechanical properties of two-dimensional layers of liquid Helium adsorbed on a substrate [3] and have characterized the universal jump of the superfluid fraction at the BKT critical point. On the other hand, liquid helium experiments have limited access to the momentum distribution and the correlation functions of the fluid. The situation of ultracold-atom experiments is almost the opposite: Evidence of the BKT transition has been obtained from the coherence functions [4], the number of observed vortices [5], and the density profile after time of flight [6], while the macroscopic mechanical properties of the fluid have not been characterized yet.

Recently, much effort has been devoted to the conceptual problem of how to experimentally detect genuine superfluidity in a quantum gas of ultracold atoms and not simply Bose-Einstein condensation [7]. A possibility explored in Ref. [8] is to look at the response of a gas in a toroidal trap to a static azimuthal artificial gauge field: A spectroscopic signature is proposed which should provide direct information on the total superfluid mass of the system. A different strategy proposed in Ref. [9] consists of looking at the evolution of the equilibrium density profile of a trapped gas when it is set into rotation.

In the present article we propose two experimental protocols to measure the normal fraction of a gas in a *local* way to extract its spatial dependence in a trapped geometry. This feature is most relevant for atomic samples, as the superfluid core coexists with an external ring of normal gas [10]. In particular, the proposed diagnostic technique does not require us to relate experimental observations after time of flight to in-trap quantities. Furthermore, in contrast to Ref. [9], our technique does not require thermodynamic equilibrium in the gas in presence of rotation [11] and may be applied to more general, nonequilibrium conditions.

The idea of our proposal is based on the definition of normal and superfluid fractions of a quantum fluid in terms of its current response to a transverse gauge field in the low-frequency and long-wavelength limit [14,15]. A spatially oscillating artificial gauge field [16–19] with a spatially localized envelope can be applied to the atomic gas using a suitable combination of laser beams. The response of the fluid to the gauge field can be detected either mechanically or optically. In the former case, one has to measure the amount of energy that is deposited in the atomic gas at the end of a suitable temporal sequence of gauge field. In the latter case, one can observe, e.g., the phase shift that is experienced by the laser fields while crossing the atomic cloud.

The structure and the main results of the article can be summarized as follows. In Sec. II, we review the definition of the normal and superfluid fractions that we adopt throughout the whole article. A strategy to generate the artificial gauge field with the suitable spatial geometry is presented in Sec. III using three laser beams, namely a coupling beam and two probe beams.

The first method to measure the normal fraction is by mechanical means. It is discussed in Sec. IV: A pulse of spatially modulated gauge field is suddenly applied to the gas and then slowly switched off according to an exponential law in time. An analytical calculation within the linear response theory and local-density approximation shows that the energy that is deposited in the gas at the end of the gauge-field pulse is indeed proportional to the normal (total) density in the small fraction of the gas where the probe beam is focused, if the spatial modulation of the gauge field

is orthogonal (parallel) to the coupling beam direction of propagation. Some of the complications that naturally occur in experiments are then numerically investigated: A Bogoliubov theory is used to assess the conditions to be imposed to the geometry and the temporal duration of the pulse, and a classical field model is used to assess the conditions on the amplitude of the gauge field for the linear response theory to be valid. A main difficulty appears to be the relatively small amount of energy that can be deposited in the gas before nonlinear couplings become difficult to extrapolate out: The resulting figure is on the order of 1% of the total energy of the gas, which is, however, not far from the sensitivity of state-of-the-art thermodynamic measurements of the energy [20–24].

The second method to measure the normal fraction is by optical means. It is discussed in Sec. V A. The spatially modulated gauge field is imposed using the same laser beam configuration in a continuous-wave regime to generate a stationary current pattern in the gas. This current pattern can be read out from the phase shift accumulated by the same probe laser beams after crossing the atomic cloud. Analytical calculations show that this phase shift is indeed proportional to the normal (total) density if the spatial modulation of the gauge field is orthogonal (parallel) to the coupling beam direction of propagation. For realistic configurations, the amount of the phase shift is anticipated to be of the order of a fraction of 10^{-3}, i.e., small but still appreciable with present-day optical techniques.

Another optical setup that is able to provide quantitative information on the normal fraction is discussed in Sec. V B: Analytical calculations are used to relate the angular distribution of the scattered light off a single probe beam to the normal fraction of the gas. The main advantage of this last configuration is the rapidity of the measurement but the limiting factor is the relatively small number of photons (of the order of a few units) that are expected to be scattered in the useful directions.

In Appendix A we discuss how to cope with all those spurious effects that arise from a realistic configuration of atomic levels and laser fields, in particular, spontaneous emission and the mechanical effect of undesired light shifts. Even though the underlying concepts are general, the discussion is mostly focused on the most promising case of ^{87}Rb atoms. The generalization of the Dum-Olshanii theory of artificial gauge fields to the many-body context is reported in Appendix B: This development is required to put the gauge-field concepts on firm ground in presence of atomic interactions and to evaluate in a rigorous way the optical response of the atoms to the combined coupling and probe beams. Appendix C gives more details on the analytical derivation of the deposited energy and clarifies some issues related to the local-density approximation. The framework for calculating the deposited energy using the Bogoliubov theory within the linear response regime is discussed in Appendix D. The last Appendix, Appendix E, discusses issues related to the statistical noise on the deposited energy both in the numerical calculation and in an actual experiment. In particular, it shows how useful information on the normal fraction could be extracted from the noise if a sufficiently precise determination of the initial energy was possible. We conclude in Sec. VI.

II. DEFINITION OF SUPERFLUID AND NORMAL FRACTIONS

Our proposal to quantitatively assess the superfluidity of the two-dimensional atomic gas is based on the traditional definition of the normal fraction f_n in terms of the response to a transverse gauge-field coupling to the atomic current operator [14,15]. The Hamiltonian giving the coupling of the matter current to an arbitrary vector potential $\mathbf{A}(\mathbf{r})$ is

$$V = -\int d^2\mathbf{r}\, \mathbf{A}(\mathbf{r}) \cdot \mathbf{j}(\mathbf{r}), \tag{1}$$

with the current operator defined as usual as

$$\mathbf{j}(\mathbf{r}) = \frac{\hbar}{2im}[\hat{\phi}^\dagger(\mathbf{r})\nabla\hat{\phi}(\mathbf{r}) - \text{H.c.}] \tag{2}$$

in terms of the bosonic field operator $\hat{\phi}$ for the two-dimensional gas. For a spatially homogeneous system, the linear response susceptibility relating the average current [25] to the applied gauge field can be easily written in momentum space and frequency domain as

$$\langle\mathbf{j}\rangle(\mathbf{q},\omega) = \chi(\mathbf{q},\omega)\,\mathbf{A}(\mathbf{q},\omega). \tag{3}$$

If the system is also invariant under reflection with respect to the direction of $\mathbf{q}$, the susceptibility tensor $\chi(\mathbf{q},\omega)$ turns out to be diagonal in the longitudinal/transverse basis with respect to $\mathbf{q}$, with diagonal matrix elements $\chi_{L,T}(\mathbf{q},\omega)$, respectively.

For a system of surface density ρ, the normal fraction f_n of the system is then defined as the low-momentum, low-frequency limit of the susceptibility to transverse gauge fields as follows:

$$f_n = \lim_{q\to 0}\lim_{\omega\to 0}\frac{m}{\rho}\chi_T(\mathbf{q},\omega). \tag{4}$$

Note that the order of the limits is important. A well-known sum rule based on gauge invariance imposes that the same limit for the longitudinal susceptibility $\chi_L(\mathbf{q},\omega)$ gives exactly unity,

$$1 = \lim_{q\to 0}\lim_{\omega\to 0}\frac{m}{\rho}\chi_L(\mathbf{q},\omega). \tag{5}$$

Equation (4) can then be extended to large but finite systems using the standard local-density approximation.

III. HOW TO GENERATE THE GAUGE FIELD

We consider a three-dimensional gas of bosonic atoms in a strongly anisotropic, pancake-shaped trap. The axial confinement frequency ω_z is much higher than the one $\omega_\parallel$ along the xy plane; both the temperature T (times the Boltzmann constant k_B) and the chemical potential μ of the gas are assumed to be smaller than $\hbar\omega_z$. In this regime, the gas will be eventually described in terms of a two-dimensional Hamiltonian.

Building on an idea originally introduced in Ref. [16], an artificial gauge-field coupling to the atomic current can be obtained by illuminating the atoms with several laser beams with suitably chosen frequencies, wave vectors, and waist profiles. Several schemes to generate artificial gauge fields for neutral atoms have been proposed in the last years [16–18]. The last proposal [18] was recently implemented on an atomic
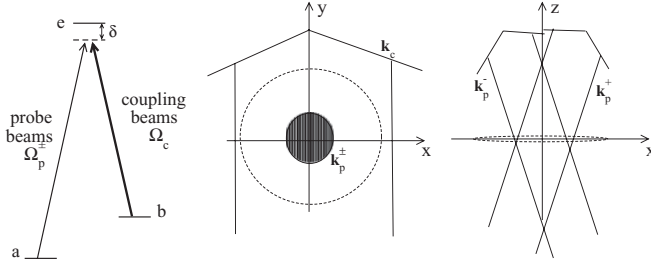
FIG. 1. Scheme of the setup under consideration. (Left panel) Generic sketch of the Λ configuration of atomic levels and laser beams involved in the optical processes. (Center panel) View from above of the two-dimensional atomic pancake (lying within the dashed circle) and of the laser beams (the hatched disk is the spot of the probe beams in the xy plane). (Right panel) Side view. $\mathbf{k}_c$ and $\mathbf{k}_p^\pm$ are the wave vectors of the coupling and probe beams, respectively. In practice, $\mathbf{k}_p^\pm = (k_p^2 - q^2/4)^{1/2}\,\mathbf{e}_z \pm (q/2)\,\mathbf{e}_x$ with $q \ll k_p$, where $\mathbf{e}_i$ is the unit vector along axis i.

Bose-Einstein condensate: For sufficiently strong gauge fields, a disordered ensemble of vortices appeared in the gas [19].

In the present article, we focus our attention on the level configuration shown in Fig. 1. Three internal atomic levels in a Λ configuration are connected by three laser fields according to the sketch given in the left panel of Fig. 1: A coupling beam resonantly drives the $|b\rangle \rightarrow |e\rangle$ atomic transition, while a pair of probe beams resonantly drive the $|a\rangle \rightarrow |e\rangle$ transition with essentially the same detuning. The artificial gauge field originates from the spatial and temporal dependence of the resulting optically dark state [16]. All other atomic states are assumed to be far-off resonance. A discussion of their effect in the specific case of ^{87}Rb atoms is given in Appendix A. A summary of the suggested experimental parameters for this specific atomic species is given in Table I.

The geometrical arrangement of the laser beams is sketched in the central and right panels of Fig. 1. The continuous-wave control beam propagates along the y direction with a wave vector $\mathbf{k}_c$ and a carrier frequency ω_c close to resonance with the $|b\rangle \rightarrow |e\rangle$ transition, with a detuning δ, and has a peak Rabi frequency Ω_c^o. Its waist profile is much wider than the size of the atomic cloud, so it can be safely approximated by a plane wave.

The two probe beams share the same carrier frequency ω_p close to resonance with the $|a\rangle \rightarrow |e\rangle$ transition. The carrier frequencies of the coupling and probe beams are chosen exactly on resonance with the Raman transition $|a\rangle \rightarrow |e\rangle \rightarrow |b\rangle$, that is, $\omega_p - \omega_c = \omega_b - \omega_a$. The probe beams impinge on the atomic cloud with wave vectors $\mathbf{k}_p^\pm \simeq k_p \mathbf{e}_z \pm \mathbf{q}/2$ close to the z direction and symmetrically located with respect to it. The difference $\mathbf{q} = \mathbf{k}_p^+ - \mathbf{k}_p^-$ lies along the xy plane and is in magnitude $q \ll k_p = \omega_p/c$. The probe beams spatial profile is taken to be a Gaussian with a waist w, centered at $\mathbf{r}_0$ in the $z = 0$ plane.

In what follows, we will need the condition $w \gg q^{-1}$, where q is small enough for the limit in Eq. (4) to be almost reached. In the numerical examples to come, this requires $q\xi < 1$, where ξ is the healing length of the gas. This automatically shows that the concept of normal fraction can be used only when the portion of the gas within the waist is "macroscopic" [26], here $w \gg \xi$, which was physically expected. At

TABLE I. Suggested values of the physical parameters for an experimental measurement of the normal fraction of a two-dimensional Bose gas of ^{87}Rb using an artificial gauge field produced by laser (coupling and probe beam) excitation on the D1 line with an optical wavelength $\lambda_c = 795$ nm. The first block characterizes the thermal equilibrium of the gas. The second block determines the gauge field. The third block deals with the issues of spontaneous emission and spurious light shift for two atomic level schemes: The "first choice" is Fig. 6(a), and the "second choice" is Fig. 6(b). For this second choice, the indicated value $|\Omega_c|^2/\Gamma^2 = 0.5$ corresponds to a compromise between minimization of the fluorescence and of the spurious light shift, the truly minimal P_{fluo} being < 0.01, see (A18). Note that P_{fluo} and $\Delta E_U/\Delta E_2$ are basically unchanged if one takes $q\xi = 1/2$ and $\gamma/(c_s q) = 0.4$. The three-dimensional scattering length $a_{3D} \simeq 100$ Bohr radii is related to the two-dimensional coupling constant by Eq. (20). A useful relation is $m\Gamma/(\hbar k_c^2) \simeq 792$; $c_s = (\rho g/m)^{1/2}$ is the Bogoliubov sound velocity.

2D density	$\rho\lambda_c^2 = 9$	$\rho = 14\ \mu\text{m}^{-2}$
Degeneracy temperature	$k_B T_d \equiv 2\pi\hbar^2\rho/m$	$T_d = 500$ nK
Temperature	$T = 0.1\,T_d$	$T = 50$ nK
2D interaction constant	$\tilde{g} = mg/\hbar^2$	$\tilde{g} = 0.1$
Transverse confinement	$\hbar\omega_z = 0.23\,\hbar^2 k_c^2/m$ $= 0.16\,k_B T_d$	$\frac{\omega_z}{2\pi} = 1.65$ kHz
Healing length	$\xi \equiv (\rho\tilde{g})^{-1/2}$	$\xi = 0.84\ \mu\text{m}$
Reduced gauge field amplitude	$\tilde{\epsilon}_{\text{gauge}} \equiv \frac{\epsilon_{\text{gauge}}}{(mk_B T_d)^{1/2}}$	$\tilde{\epsilon}_{\text{gauge}} = 0.15$
Probe beam Rabi frequencies	$\frac{(|\Omega_p^+|^2 + |\Omega_p^-|^2)_{t=0^+}}{2|\Omega_c|^2}$	0.09
Gauge field switch-off rate	$\gamma = 0.2\,c_s q$ with $q = 1/\xi$	$1/\gamma = 4.8$ ms $q = 0.15 k_c$

Level schemes of Fig. 6	First choice	Second choice
Level $|a\rangle$	$|F = 1, -1\rangle$	$|F = 2, -2\rangle$
Level $|b\rangle$	$|F = 2, -2\rangle$	$|F = 1, -1\rangle$
Level $|e\rangle$	$|F' = 2, -1\rangle$	$|F' = 2, -2\rangle$
Squared coupling Rabi frequency $|\Omega_c|^2/\Gamma^2$	0.21	0.5
Minimum detuning δ/Γ	1	1.5
Fluorescence atom probability per P_{fluo}	0.22	0.045
Spurious deposited energy $\Delta E_U/\Delta E_2$ (for $f_n = 0.2$)	33	0.16

the same time, the waist w is assumed to be much smaller than the atomic cloud radius, to allow for a local measurement of the normal fraction. The peak Rabi frequencies of the two probe beams are $\Omega_p^\pm(t)$, respectively (see Appendix B for the precise definition of the Rabi frequencies). The spatial dependence of the Rabi frequencies of both the coupling and the probe beams is then summarized by the following expressions [27]:

$$\Omega_c(\mathbf{r},t) = \Omega_c^{(0)} e^{-i\Delta_c t}\, e^{i\mathbf{k}_c\cdot\mathbf{r}}, \qquad (6)$$

$$\Omega_p(\mathbf{r},t) \simeq [\Omega_p^+(t)\,e^{i\mathbf{k}_p^+\cdot\mathbf{r}} + \Omega_p^-(t)\,e^{i\mathbf{k}_p^-\cdot\mathbf{r}}]$$
$$\times\, e^{-[(x-x_0)^2+(y-y_0)^2]/w^2}, \qquad (7)$$

where we have allowed for the coupling beam to have a small detuning Δ_c from Raman resonance on top of its carrier frequency at ω_c. On the contrary, Ω_p does not have a time-dependent phase factor but contains only the square root of a purely real non-negative switch-on and switch-off function $f(t)$, common to the two probe beams as follows:

$$\Omega_p(\mathbf{r},t) = \Omega_p^0(\mathbf{r})[f(t)]^{1/2}. \qquad (8)$$

In what follows, we shall restrict our attention to the nonsaturating regime $|\Omega_c|, |\Omega_p^\pm| \ll |\delta + i\Gamma/2|$, where Γ is the decay rate of $|e\rangle$ due to spontaneous emission and δ is the common detuning of the probe and control beam carrier frequencies from the transitions $|a\rangle \to |e\rangle$ and $|b\rangle \to |e\rangle$, respectively. We shall also concentrate on the limit $|\Omega_p^\pm| \ll |\Omega_c|$ where the structure of the gauge field is the simplest.

As the transitions driven by the probe and control beams share the excited state $|e\rangle$, there exists for each spatiotemporal coordinates $(\mathbf{r},t)$ an internal *noncoupled state*, for which the two excitation channels interfere destructively. In terms of the local Rabi frequencies $\Omega_p(\mathbf{r},t)$ and $\Omega_c(\mathbf{r},t)$, this noncoupled state reads

$$|NC(\mathbf{r},t)\rangle = \frac{|a\rangle - \Omega_p(\mathbf{r},t)/\Omega_c(\mathbf{r},t)\,|b\rangle}{[1 + |\Omega_p(\mathbf{r},t)|^2/|\Omega_c(\mathbf{r},t)|^2]^{1/2}}. \qquad (9)$$

Adiabatically eliminating the excited state $|e\rangle$, one sees that the bright orthogonal state, the so-called coupled state,

$$|C(\mathbf{r},t)\rangle = \frac{[\Omega_p(\mathbf{r},t)/\Omega_c(\mathbf{r},t)]^*|a\rangle + |b\rangle}{(1 + |\Omega_p(\mathbf{r},t)|^2/|\Omega_c(\mathbf{r},t)|^2)^{1/2}}, \qquad (10)$$

is separated from $|NC(\mathbf{r},t)\rangle$ by a (complex) energy gap

$$\hbar[\delta'(\mathbf{r},t) - i\Gamma'(\mathbf{r},t)/2] \equiv \frac{\hbar[|\Omega_c(\mathbf{r},t)|^2 + |\Omega_p(\mathbf{r},t)|^2]}{4(\delta + i\Gamma/2)}, \quad (11)$$

where δ' and Γ' are the light shift and the decay rate of the coupled state. If the energy gap is large enough as compared to both the motional coupling between $|NC\rangle$ and $|C\rangle$ due to the spatiotemporal dependence of Ω_c and $\Omega_p^\pm$ [28], and to the quantum of oscillation $\hbar\omega_z$ along the tightly confined z direction, we can restrict the dynamics to the $|NC\rangle$ internal state.

Generalizing the single-particle theory of Ref. [16] to the many-body context in Heisenberg picture, one gets to an effective Hamiltonian for the component $\hat{\phi}_{3D}(\mathbf{r},t)$ of the three-dimensional atomic field operator in the (spatially and temporally dependent) noncoupled state $|NC(\mathbf{r},t)\rangle$,

$$\hat{\phi}_{3D}(\mathbf{r},t) = \langle NC(\mathbf{r},t)|a\rangle\,\hat{\Psi}_a(\mathbf{r},t) + \langle NC(\mathbf{r},t)|b\rangle\,\hat{\Psi}_b(\mathbf{r},t) \quad (12)$$

in the simple form [29]:

$$\mathcal{H} = \int d^3\mathbf{r}\,\left\{ \hat{\phi}_{3D}^\dagger\left[-\frac{\hbar^2\nabla^2}{2m} + U_{3D}(\mathbf{r}) + W_{3D}(\mathbf{r},t)\right]\hat{\phi}_{3D} \right.$$
$$\left. -\,\mathbf{j}_{3D}(\mathbf{r})\cdot\mathbf{A}_{3D}(\mathbf{r},t) + \frac{1}{2}g(\mathbf{r},t)\,\hat{\phi}_{3D}^\dagger\hat{\phi}_{3D}^\dagger\hat{\phi}_{3D}\hat{\phi}_{3D} \right\}, \quad (13)$$

where U_{3D} is the three-dimensional trapping potential (supposed to be common to the internal states $|a\rangle$ and $|b\rangle$) and the vector gauge potential

$$\mathbf{A}_{3D}(\mathbf{r},t) = \frac{i\hbar}{2}\{\langle NC(\mathbf{r},t)|[\nabla|NC(\mathbf{r},t)\rangle] - \text{c.c.}\} \qquad (14)$$

couples to the three-dimensional atomic current operator

$$\mathbf{j}_{3D}(\mathbf{r}) = \frac{\hbar}{2im}[\hat{\phi}_{3D}^\dagger(\mathbf{r})\nabla\hat{\phi}_{3D}(\mathbf{r}) - \text{H.c.}], \qquad (15)$$

and the scalar potential

$$W_{3D}(\mathbf{r},t) = -\frac{i\hbar}{2}\{\langle NC(\mathbf{r},t)|\,[\partial_t|NC(\mathbf{r},t)\rangle] - \text{c.c.}\}$$
$$+ \frac{\hbar^2}{2m}\sum_{i=x,y,z}[\partial_{r_i}\langle NC(\mathbf{r},t)|][\partial_{r_i}|NC(\mathbf{r},t)\rangle] \quad (16)$$

couples to the three-dimensional density

$$n_{3D}(\mathbf{r}) = \hat{\phi}_{3D}^\dagger(\mathbf{r})\,\hat{\phi}_{3D}(\mathbf{r}). \qquad (17)$$

The derivation of Hamiltonian (13) is based on the quantum stochastic differential equations formalism [30]; the details are given in Appendix B.

The spatial and temporal dependence of the weights of the noncoupled state (9) in the internal states $|a\rangle$ and $|b\rangle$ reflects into a similar variation of the coupling constant describing the atomic interaction within the internal state $|NC\rangle$:

$$g_{3D}(\mathbf{r},t) = \frac{|\Omega_c|^4\,g_{aa} + 2|\Omega_p(\mathbf{r},t)|^2\,|\Omega_c|^2\,g_{ab} + |\Omega_p|^4\,g_{bb}}{(|\Omega_c|^2 + |\Omega_p(\mathbf{r},t)|^2)^2}, \quad (18)$$

where the coupling constants g_{aa}, g_{ab}, and g_{bb} originate from the a-a, a-b, and b-b elastic s-wave interactions. In what follows, we shall be interested in isolating the response of the system to the gauge field $\mathbf{A}_{3D}$. To this purpose, it will be useful to minimize the effect of all unwanted couplings to the density introduced by the scalar potential W_{3D} and by the spatiotemporal dependence of the interaction constant g_{3D}. This latter effect is minimized if one chooses states a,b with similar scattering properties $g_{aa} \simeq g_{ab} \simeq g_{bb}$. In the limit $|\Omega_p/\Omega_c| \ll 1$, one simply needs to have $g_{aa} \simeq g_{ab}$, as it is assumed from now on.

The atomic field along z is assumed to be frozen in the ground state of the harmonic confinement of wave function $\phi_0(z)$. This allows us to express the three-dimensional bosonic field $\hat{\phi}_{3D}$ in terms of the bosonic field for a two-dimensional gas, setting

$$\hat{\phi}_{3D}(x,y,z) = \phi_0(z)\hat{\phi}(x,y). \qquad (19)$$

Correspondingly, the two-dimensional coupling constant g has the expression

$$g = \frac{\hbar^2}{m}\tilde{g} = \frac{g_{3D}}{\sqrt{2\pi}\,a_{\text{ho}}^z} \qquad (20)$$

in terms of the three-dimensional coupling constant $g_{3D} = 4\pi\hbar^2 a_{3D}/m$, where a_{3D} is the s-wave scattering length in the state $|a\rangle$, and the size $a_{\text{ho}}^z = \sqrt{\hbar/m\omega_z}$ of the ground state along z. Note that the dimensional reduction (19) does not require us to be in the Lamb-Dicke limit $k_{p,c}a_{\text{ho}}^z \ll 1$; it is sufficient that the typical energy per particle corresponding to the various

terms in $\mathcal{H}$ (other than the harmonic oscillator Hamiltonian along z) is $\ll \hbar\omega_z$.

The effective two-dimensional gauge and scalar potentials **A** and W then result from an average of the Hamiltonian (13) over the motional ground state along z. Including in Eqs. (14) and (16) the explicit form of the beam profiles and restricting ourselves to zeroth order in the small parameters $q/k_{p,c}$ and $1/wk_{p,c}$, and to second order in $\Omega_p^\pm/\Omega_c$, the resulting two-dimensional gauge potential turns out to be directed along the y axis and to have the form

$$
\begin{aligned}
A_y(\mathbf{r}) &\simeq \hbar k_c \frac{|\Omega_p^+ e^{i\mathbf{q}\cdot\mathbf{r}/2} + \Omega_p^- e^{-i\mathbf{q}\cdot\mathbf{r}/2}|^2}{|\Omega_c|^2} e^{-2|\mathbf{r}-\mathbf{r}_0|^2/w^2} \\
&= \hbar k_c \frac{|\Omega_p^+|^2 + |\Omega_p^-|^2 + [\Omega_p^+ \Omega_p^{-*} e^{i\mathbf{q}\cdot\mathbf{r}} + \text{c.c.}]}{|\Omega_c|^2} \\
&\quad \times e^{-2|\mathbf{r}-\mathbf{r}_0|^2/w^2}.
\end{aligned}
\tag{21}
$$

To the same level of approximation, the scalar potential has the form

$$
\begin{aligned}
W(\mathbf{r}) &= \left[\frac{\hbar^2(k_c^2 + k_p^2)}{2m} + \hbar\Delta_c \right] \frac{|\Omega_p^+ e^{i\mathbf{q}\cdot\mathbf{r}/2} + \Omega_p^- e^{-i\mathbf{q}\cdot\mathbf{r}/2}|^2}{|\Omega_c|^2} \\
&\quad \times e^{-2|\mathbf{r}-\mathbf{r}_0|^2/w^2},
\end{aligned}
\tag{22}
$$

which can be made to vanish by choosing a detuning Δ_c that exactly compensates the recoil of the atoms after the Raman process $a \to e \to b$:

$$
W \equiv 0 \quad \text{for} \quad \Delta_c = -\frac{\hbar(k_c^2 + k_p^2)}{2m}.
\tag{23}
$$

It is worth pointing out that the temporal derivative $df(t)/dt$ of the real switch-on and switch-off function $f(t)$ of the probe beam of Eq. (8) has an exactly vanishing contribution to the ∂_t term in the right-hand side of Eq. (16), so it does not contribute to the scalar potential W to all orders in Ω_p/Ω_c [31]. The same conclusion holds for the gauge field, since there is no temporal derivative in Eq. (14).

After expansion of the squared modulus as done in the second line of Eq. (21), two kinds of terms are immediately identified: (i) a slowly varying Gaussian term of size w and peak amplitude $|\Omega_p^+|^2 + |\Omega_p^-|^2$ that follows the laser envelopes and (ii) an oscillating term at wave vector **q** with a Gaussian envelope of size w and peak amplitude $|\Omega_p^+ \Omega_p^-|$. This spatially modulated term is indeed the one that we need to probe the normal fraction of the gas according to Eq. (4): When **q** is taken along the x axis (y axis), it provides an almost purely transverse (longitudinal) contribution to the gauge field **A**. On the other hand, the slowly varying term always includes both longitudinal and transverse vector field components. Experimental procedures to subtract the effect of this unwanted term will be discussed in the next sections.

IV. DEPOSITED ENERGY MEASUREMENT

A. General idea

In this section we shall present a method to extract the value of the normal fraction from a measurement of the energy that is deposited in the system by a suitably designed gauge-field sequence. The coupling beam is assumed to be always switched on. On the other hand, both probe beam intensities $|\Omega_p^\pm|^2$ are varied in time according to the (dimensionless) real envelope function $f(t)$. This function is chosen to be 0 for $t < 0$ and to rapidly tend back to 0 at long times.

As already mentioned, we assume that the atomic interaction constants satisfy $g_{aa} \simeq g_{ab}$ [32]. As soon as $qw \gg 1$, the deposited energy is the sum of two independent contributions $\Delta E_{1,2}$ corresponding to the decomposition (21) of the gauge field as the sum of a nonmodulated term and a modulated one at the wave vector **q**. Using standard linear response theory within the local-density approximation as discussed in the Appendix C, the contribution ΔE_2 of the modulated term can be written in the simplified form

$$
\Delta E_2 \simeq \frac{\pi}{4} w^2 \left(\frac{\epsilon_{\text{gauge}}}{2} \right)^2 \int_{-\infty}^{+\infty} \frac{d\omega}{\pi} \, \omega \, |f(\omega)|^2 \, \text{Im}[\chi_{yy}(\mathbf{q},\omega)],
\tag{24}
$$

where we have introduced the amplitude of the spatially modulated part of the gauge field,

$$
\epsilon_{\text{gauge}} = 2\hbar k_c \frac{|\Omega_p^+ \Omega_p^-|(t = 0^+)}{|\Omega_c|^2}.
\tag{25}
$$

A similar expression for the contribution ΔE_1 of the non-modulated term is given in the Appendix C as (C8). The susceptibility χ_{yy} appearing in expression (24) is the one (as defined in Sec. II) of the fictitious spatially homogeneous two-dimensional Bose gas that approximates the state of the trapped gas around the center $\mathbf{r}_0$ of the probe beams' spot.

The expression (24) for the deposited energy involves the imaginary part of that susceptibility, while the normal fraction [Eq. (4)] involves the real part. To relate the two, one can make use of the well-known Kramers-Kronig relation of linear response theory,

$$
\lim_{\omega\to 0} \text{Re}[\chi(\mathbf{q},\omega)] = \int_{-\infty}^{+\infty} \frac{d\omega'}{\pi} \frac{\text{Im}[\chi(\mathbf{q},\omega')]}{\omega'}.
\tag{26}
$$

For a suitably chosen envelope of the form

$$
f(t) = e^{-\gamma t} \, \Theta(t),
\tag{27}
$$

where $\Theta(t)$ is the Heaviside step function, the Fourier transform is equal to $f(\omega) = i/(\omega + i\gamma)$, and the integral in expression (24) indeed reduces to the real part of the susceptibility [Eq. (26)] in the $\gamma \to 0$ limit.

As a consequence, the deposited energy ΔE_2 for small **q** perpendicular (parallel) to $\mathbf{k}_c$ can be related to the normal (total) density ρ_n (ρ) of the trapped gas at position $\mathbf{r}_0$ by

$$
\Delta E_2 \simeq \frac{\pi}{4} \frac{w^2}{m} \left(\frac{\epsilon_{\text{gauge}}}{2} \right)^2 \begin{cases} \rho_n(\mathbf{r}_0) & \text{for} \quad \mathbf{q} \perp \mathbf{k}_c \\ \rho(\mathbf{r}_0) & \text{for} \quad \mathbf{q} \parallel \mathbf{k}_c \end{cases}.
\tag{28}
$$

For intermediate angles α between **q** and $\mathbf{k}_c$, ΔE_2 is proportional to $\rho \cos^2\alpha + \rho_n \sin^2\alpha$ [34].

In an actual experiment, the undesired contribution ΔE_1 can be eliminated by noting its independence on the relative orientation of **q** and $\mathbf{k}_c$ [see Eqs. (C8) and (C9)], as well as its different dependence on the probe amplitudes $\Omega_p^\pm$, proportional to $[|\Omega_p^+|^2 + |\Omega_p^-|^2]^2$ rather than $|\Omega_p^+ \Omega_p^-|^2$. By measuring the deposited energy for at least two different values of the Ω_p^+/Ω_p^- ratio, one is able to isolate the relevant contribution (28).

B. How fast is the $q,\gamma \to 0$ limit reached?

An important point in view of experiments is to characterize how small the wave number q and the switch-off rate γ of the gauge-field spatial modulation have actually to be taken to obtain a quantitatively accurate measurement of the normal fraction f_n. To answer this question, we consider in this subsection the simplest case of a spatially homogeneous two-dimensional system in a square box of size L with periodic boundary conditions, excited by the gauge field in a plane-wave form, i.e., in the limit $w \to \infty$. We also limit ourselves to the case of a transverse gauge field with $\mathbf{q} = q\,\mathbf{e}_x$ perpendicular to $\mathbf{k}_c = k_c\,\mathbf{e}_y$,

$$\mathbf{A}_{\text{ideal}}(\mathbf{r},t) = e^{-\gamma t}\,\Theta(t)\mathbf{e}_y\,\frac{\epsilon_{\text{gauge}}}{2}(e^{iqx} + e^{-iqx}). \tag{29}$$

The deposited energy at the end of the gauge-field sequence can be evaluated by means of the Bogoliubov theory of dilute Bose gases. The main steps of the calculation are outlined in Appendix D. The final result reads

$$\Delta E_2 = \left(\frac{\epsilon_{\text{gauge}}}{2}\right)^2 \frac{N}{m} f_n^{\text{eff}} \tag{30}$$

in terms of the wave vector- and γ-dependent effective normal fraction f_n^{eff}:

$$f_n^{\text{eff}} = \frac{1}{N} \sum_{\mathbf{k}\neq \mathbf{0},-\mathbf{q}} \frac{\hbar^2 k_y^2}{m} \text{Re}\Bigg[\frac{n_{\mathbf{k}} - n_{\mathbf{k}+\mathbf{q}}}{\epsilon_{\mathbf{k}+\mathbf{q}} - \epsilon_{\mathbf{k}} - i\hbar\gamma}(U_{\mathbf{k}}U_{\mathbf{k}+\mathbf{q}}$$
$$- V_{\mathbf{k}}V_{\mathbf{k}+\mathbf{q}})^2 + \frac{1 + n_{\mathbf{k}} + n_{\mathbf{k}+\mathbf{q}}}{\epsilon_{\mathbf{k}+\mathbf{q}} + \epsilon_{\mathbf{k}} - i\hbar\gamma}(U_{\mathbf{k}}V_{\mathbf{k}+\mathbf{q}} - V_{\mathbf{k}}U_{\mathbf{k}+\mathbf{q}})^2\Bigg]. \tag{31}$$

Here N is the total particle number, $\rho = N/L^2$ is the surface density,

$$\epsilon_{\mathbf{k}} = \left[\frac{\hbar^2 k^2}{2m}\left(\frac{\hbar^2 k^2}{2m} + 2\rho g\right)\right]^{1/2} \tag{32}$$

is the usual Bogoliubov dispersion relation and the amplitudes of the Bogoliubov modes satisfy

$$U_{\mathbf{k}} + V_{\mathbf{k}} = \frac{1}{U_{\mathbf{k}} - V_{\mathbf{k}}} = \left(\frac{\hbar^2 k^2/2m}{\hbar^2 k^2/2m + 2\rho g}\right)^{1/4}. \tag{33}$$

The $n_{\mathbf{k}}$ are the thermal mean occupation numbers of Bogoliubov modes, $n_{\mathbf{k}} = 1/[\exp(\epsilon_{\mathbf{k}}/k_B T) - 1]$.

The thermodynamic limit $L \to \infty$ at fixed density N/L^2 can be worked out analytically by first taking the $\gamma \to 0$ limit and then the $q \to 0$ limit in the expression (31) for f_n^{eff}. In this way one recovers the usual Bogoliubov expression for the normal fraction, which in dimension 2 reads:

$$f_n = \frac{1}{\rho} \int \frac{d^2 k}{(2\pi)^2} \frac{\hbar^2 k_y^2}{m}(-\partial_{\epsilon_{\mathbf{k}}} n_{\mathbf{k}}). \tag{34}$$

For a finite-size system, the dependence of f_n^{eff} on γ and q is explored in Fig. 2. For the smallest nonzero wave-vector value allowed by the chosen quantization box, the relative error on f_n^{eff} is already as small as 10% for $\gamma/c_s q = 0.15$, where $c_s = (\rho g/m)^{1/2}$ is the Bogoliubov sound velocity. For $\gamma/(c_s q)$ fixed, in particular to the relevant value 0.2, and over the relevant range $q\xi \leqslant 1$, we have also found that f_n^{eff} is to a
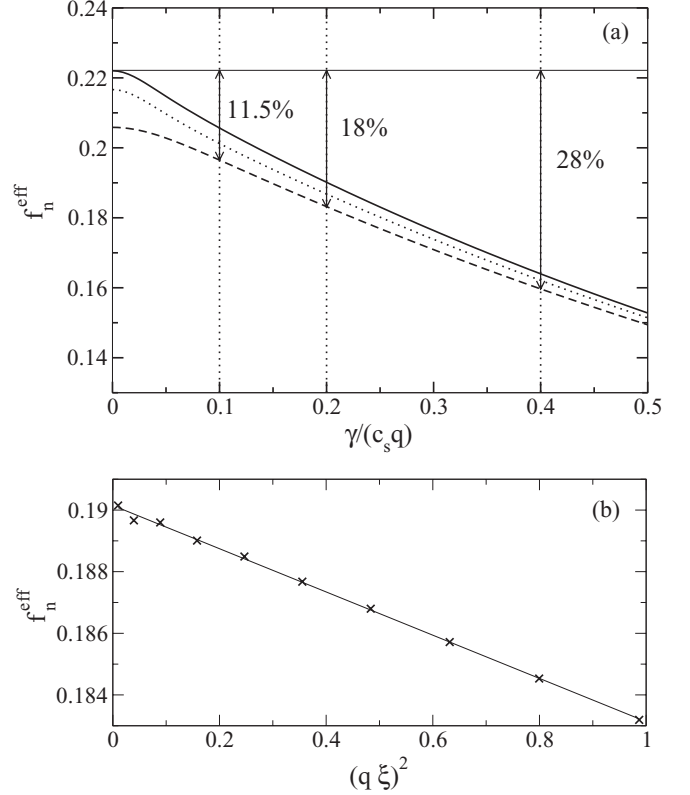

FIG. 2. Quantum Bogoliubov prediction (31) for the effective normal fraction f_n^{eff}. In (a), dependence of f_n^{eff} on the switch-off rate γ of the gauge field for three different values of the gauge-field spatial-modulation wave vector $\mathbf{q} = (2\pi/L)\,\mathbf{e}_x$ (solid line, $q\xi \simeq 0.1$), $\mathbf{q} = 7 \times (2\pi/L)\,\mathbf{e}_x$ (dotted line, $q\xi \simeq 0.7$) and $\mathbf{q} = 10 \times (2\pi/L)\,\mathbf{e}_x$ (dashed line, $q\xi \simeq 1$). System parameters: square box (with periodic boundary conditions) of size $L/\xi \simeq 63$ containing $N \simeq 40\,000$ particles with interaction constant $g = 0.1\hbar^2/m$ at a temperature $T/T_d = 0.1$. $k_B T_d = 2\pi\hbar^2\rho/m$ is the degeneracy temperature. The healing length ξ of the gas is defined by $\hbar^2/(m\xi^2) = \rho g$ and the Bogoliubov sound velocity is defined as $c_s = (\rho g/m)^{1/2}$. The dashed curve corresponds to the same value of $q\xi \simeq 1$ as in Fig. 4 and the vertical dotted lines indicate the values of $\gamma/(c_s q)$ considered in that figure. The thin horizontal line is the prediction (34) of the quantum Bogoliubov theory in the thermodynamic limit. Interestingly, for the considered atom number, the finite-size thermodynamic formula [Eq. (39)] evaluated with the quantum Bogoliubov theory gives already the same value at the scale of the figure [35]. The quadratic rather than linear dependence of f_n^{eff} on γ for small values of γ is a finite-size effect. The fact that in (a), the values of f_n^{eff} for the dotted curve are close to the arithmetic mean of the solid and dashed curves, for common values of $\gamma/(c_s q)$, suggests that f_n^{eff} is roughly an affine function of $(q\xi)^2$ for fixed $\gamma/(c_s q)$. This guess is substantiated in panel (b) where the dependence of the effective normal fraction on the modulation wave vector $\mathbf{q} = q\,\mathbf{e}_x$ is shown for $\gamma/(c_s q) = 0.2$ [the crosses are the Bogoliubov predictions and the line is a linear fit of f_n^{eff} as a function of q^2].

good approximation an affine function of $(q\xi)^2$, see Fig. 2(b), which was not obvious.

Another interesting result of Bogoliubov theory applied to our system is a sufficient condition on the amplitude of the gauge field to be within the linear response regime. To this purpose, we can write the equations of motion for the

Bogoliubov mode operators $b_{\mathbf{k}}$ in the interaction picture in the presence of the time-dependent gauge field and impose that the amplitude change is small as compared to the initial value. The expression of this amplitude change, which we do not give here, involves, as usual, energy denominators such as $\epsilon_{\mathbf{k}} - \epsilon_{\mathbf{k} \pm \mathbf{q}} + i\hbar\gamma$.

In the limit $\gamma \to 0$, the condition of linear response is, thus, most stringent for modes of wave vector $\mathbf{k}$ such that $\epsilon_{\mathbf{k}} = \epsilon_{\mathbf{k} \pm \mathbf{q}}$, where the real part of the energy denominator can vanish. For the maximal value of k set by the thermal occupation, this leads to the sufficient condition

$$\frac{\epsilon_{\text{gauge}}}{(mk_B T_d)^{1/2}} \lesssim \left(\frac{T_d}{T}\right)^{1/2} \frac{2\hbar\gamma}{k_B T_d}, \quad (35)$$

in terms of the degeneracy temperature $k_B T_d = 2\pi\hbar^2\rho/m$. This naive argument is, however, not able to determine to which extent this condition is actually necessary. This would require a higher-order calculation which falls beyond the scope of the present work [36].

C. Numerical investigation

To further assess the validity and accuracy of our proposed scheme we have performed full scale numerical simulations of the response of a two-dimensional Bose gas at finite temperature to the complete gauge field (21), including the Gaussian envelope of the gauge field and a circular well trapping potential. A very useful tool to this purpose is the classical field model developed and applied in a number of recent works [37,38]. For this model, both the thermal equilibrium state and the temporal dynamics can, in fact, be easily addressed with standard numerical tools and provide reliable results for the physics of the degenerate Bose gas.

We consider a classical (c-number) complex field defined on a square grid. The real space lattice constant b is chosen in terms of the thermal de Broglie wavelength $\lambda = \sqrt{2\pi\hbar^2/mk_B T}$ as $b/\lambda = \sqrt{\pi/(4\zeta)}$. The specific value $\zeta \simeq 0.80$ [39] of the numerical coefficient is such that the classical field model correctly reproduces the total number of noncondensed particles for an ideal gas at zero chemical potential in the thermodynamic limit. This choice corresponds to setting the ultraviolet momentum cutoff $k_{\max} = \pi/b$ at $\hbar^2 k_{\max}^2/2m = \zeta k_B T$ in the classical field theory.

In the canonical ensemble, the thermal probability distribution for the interacting classical field follows a Boltzmann law $\delta(\|\Psi\|^2 - N) \exp(-E[\psi]/k_B T)$ with the norm-squared $\|\Psi\|^2 = b^2 \sum_{\mathbf{r}} |\Psi(\mathbf{r})|^2$ fixed to the total atom number and the discrete Gross-Pitaevskii energy functional [40] given by

$$E[\Psi] = b^2 \sum_{\mathbf{r}} \Psi^* \left[-\frac{\hbar^2}{2m}\Delta + U(\mathbf{r}) + \frac{g}{2}|\Psi|^2 \right]\Psi, \quad (36)$$

where $U(\mathbf{r})$ is the trapping potential seen by the bidimensional gas. This probability distribution can be sampled by the long time limit of an Ito stochastic differential equation with drift terms and a noise term [41,42], including projectors in order

to keep the norm-squared constant, $\|\Psi\|^2 = N$:

$$d\Psi = -\frac{1}{2} d\tau \, \mathcal{Q}_\Psi \left[-\frac{\hbar^2}{2m}\Delta\Psi + U\Psi + g|\Psi|^2\Psi \right]$$
$$+ \frac{\sqrt{k_B T}}{b} \mathcal{Q}_\Psi d\xi - \frac{M-1}{2N}k_B T \, d\tau \, \Psi, \quad (37)$$

where M is the number of grid points, $\mathcal{Q}_\Psi$ is the projector onto the subspace orthogonal to the classical field Ψ, $d\xi$ is a complex Gaussian, zero-mean, δ-correlated and temporally white noise such that $d\xi d\xi = 0$ and

$$d\xi^*(\mathbf{r}_i) \, d\xi(\mathbf{r}_j) = d\tau \, \delta_{\mathbf{r}_i, \mathbf{r}_j}. \quad (38)$$

Our numerical procedure simply consists in, first, generating a number n_{real} of independent wave functions distributed according to the thermal Boltzmann law with energy functional (36) and then to let them evolve in real time according to the discrete time-dependent Gross-Pitaevskii equation, including the gauge potential (21) [43].

As a first application of the classical field method, we have determined the normal fraction of a spatially homogeneous two-dimensional interacting gas at thermal equilibrium. This is done using the thermodynamic formula, applicable to finite-size systems with periodic boundary conditions,

$$f_n^{\text{thermo}} = \frac{\langle P_y^2 \rangle}{Nmk_B T} \quad (39)$$

which involves the thermal variance of the total momentum P_y of the gas [44,45]. The temperature dependence of the normal fraction is shown in Fig. 3 for increasing system sizes. The sudden variation around $T/T_d \simeq 0.13$ becomes sharper and sharper as the system size is increased and should eventually correspond to a discontinuous jump in the superfluid fraction at the BKT transition [1,2,46]. The slow decrease for larger values of T/T_d is instead an artifact of the ultraviolet cutoff that has to be imposed to the classical field model in any dimension $d \geqslant 2$. Indeed, the same decrease is visible also in the case of an ideal gas, for which one can show that $f_n = 1 - T/T_d + O(e^{-T_d/T} T/T_d)$ in the thermodynamic limit.

The experimental estimation of the normal fraction obtained by the deposited energy method discussed in Sec. IV A is simulated in Fig. 4. The value of the deposited energy is extracted from the classical field simulation by taking the energy difference at the end of two evolutions using the same value of $|\Omega_p^+|^2 + |\Omega_p^-|^2$ but different relative magnitudes of $\Omega_p^\pm$, $\Omega_p^- = 0$ and $|\Omega_p^+| = |\Omega_p^-|$, respectively. This protocol aims at isolating the effect of the spatially modulated gauge potential: In the linear response limit, it is able to provide the exact value of ΔE_2 alone. The effective normal fraction is then extracted from the deposited energy via expression (28), and it is plotted in Fig. 4 as a function of the gauge-field amplitude for different values of the switch-off rate $\gamma/(c_s q) = 0.4, 0.2, 0.1$ (in black, in red, and in blue from bottom to top) [$c_s = (\rho g/m)^{1/2}$ is the Bogoliubov sound velocity] and different geometries (open squares and dashed lines for the spatially homogeneous case with periodic boundary conditions and solid circles and solid lines for the circular potential well).

The ϵ_{gauge} dependence in that figure allows us to estimate the interval where the linear response approximation is reasonable,
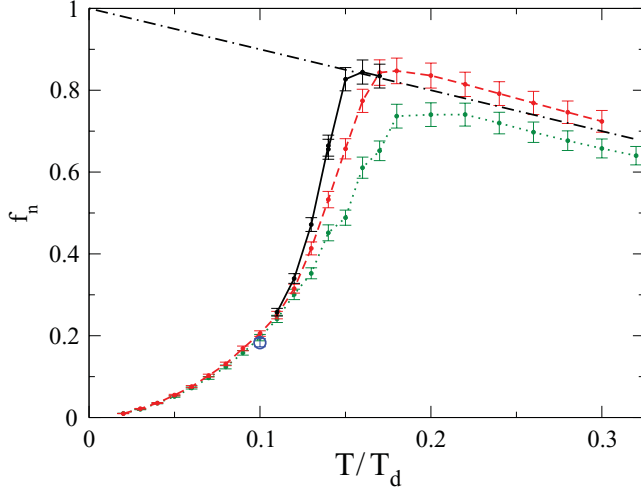
FIG. 3. (Color online) Classical field simulation of the normal fraction f_n for a finite-size two-dimensional, spatially homogeneous interacting Bose gas as a function of temperature. The calculation has been performed using the thermodynamic expression (39) for the normal fraction. The coupling constant is $g = 0.1\,\hbar^2/m$. The different curves refer to simulations performed with different system sizes L, resulting in different numbers of grid points $M = 16^2$ (dotted green line), 32^2 (dashed red line), and 64^2 (solid black line) [the grid spacing is $b \simeq 0.99\lambda$, where λ is the thermal de Broglie wavelength; see the text]. The number of classical field realizations is $n_{\text{real}} = 1000$. The dot-dashed line is the classical field prediction for the normal fraction f_n of an ideal gas in the thermodynamic limit: As discussed in the text, the decrease at high temperatures is an artifact of the classical field model. The blue circle indicates the result of a numerical simulation of the deposited energy scheme as in Fig. 4 for a homogeneous system with an infinite beam waist $w = \infty$ (in which case we simply dropped the nonmodulated term in the gauge field), a number of grid points $M = 32^2$, a gauge-field modulation wave vector $\mathbf{q} = (2\pi/L)\,\mathbf{e}_x \simeq (0.2/\xi)\,\mathbf{e}_x$, and including a careful extrapolation of $\epsilon_{\text{gauge}} \to 0$ [numerics down to $\epsilon_{\text{gauge}}/(mk_BT_d)^{1/2} = 0.01$] and of $\gamma \to 0$ [numerics down to $\gamma/(c_sq) = 0.05$, where $c_s = (\rho g/m)^{1/2}$ is the Bogoliubov sound velocity].

e.g., for $\epsilon_{\text{gauge}}/\sqrt{mk_BT_d} \lesssim 0.08$ the deviation due to nonlinear effects is less than 5% . As expected, the estimate (35) gives a more pessimistic bound around 0.04 for $\gamma/(c_sq) = 0.4$. From an experimental point of view, we expect that values of the gauge-field amplitude as high as $\epsilon_{\text{gauge}}/(mk_BT_d)^{1/2} = 0.15$ should be well achievable; see Table I. As shown in the figure, for $\epsilon_{\text{gauge}}/(mk_BT_d)^{1/2} \lesssim 0.2$, the effective normal fraction f_n empirically has, within the error bars, a linear dependence with $\epsilon_{\text{gauge}}^2$. This could be expected from the fact that the first-order correction to the linear response theory scales as $\epsilon_{\text{gauge}}^4$ in the deposited energy ΔE, the term of order $\epsilon_{\text{gauge}}^3$ in ΔE being zero due to the odd parity of the matter-wave coupling to the gauge field. Assuming this linear dependence of the effective normal fraction, a fit was performed over the range $(0.05)^2 \leqslant \epsilon_{\text{gauge}}^2/(mk_BT_d) < (0.2)^2$ to extrapolate to $\epsilon_{\text{gauge}} = 0$; see the solid and dashed lines in Fig. 4. Note that this extrapolation procedure also eliminates the contribution to the effective normal fraction of the energy ΔE_{U^p} deposited by the undesired light shifts; see the end of Appendix A. For larger values of the gauge-field amplitude ϵ_{gauge}, more serious
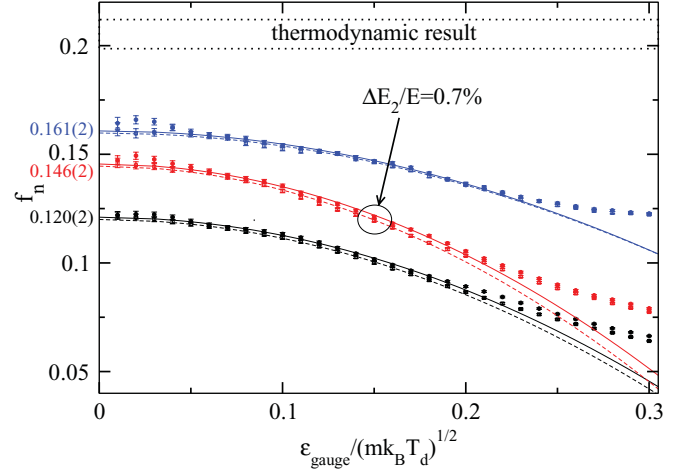

FIG. 4. (Color online) Classical field simulation of the deposited energy measurement scheme. Initial thermal equilibrium state at $T/T_d = 0.1$ with $g = 0.1\,\hbar^2/m$ and a system size $L/\xi \simeq 63$ (the number of grid points is $M = 64^2$, and $n_{\text{real}} = 1000$ independent realizations of the classical field are used). Gauge-field modulation wave vector $\mathbf{q} \simeq (1/\xi)\,\mathbf{e}_x$. The real-time evolution is followed during $\tau = 3/\gamma$. The complete form Eq. (21) of the gauge field is considered, with $\mathbf{r}_0$ located in the center of the system, and a beam waist $w = 30\xi$. For each value of the gauge-field intensity ϵ_{gauge} of Eq. (25), two calculations are performed to extract the energy change ΔE_2 due to the spatially modulated component, from which an approximate value of the normal fraction f_n is obtained (see text): the first calculation with $|\Omega_p^+|^2(0^+)/|\Omega_c|^2 = \epsilon_{\text{gauge}}/(\hbar k_c)$ and $\Omega_p^- \equiv 0$ and the second one with $|\Omega_p^{\pm}|^2(0^+)/|\Omega_c|^2 = \epsilon_{\text{gauge}}/(2\hbar k_c)$. (Open squares with error bars) Spatially homogeneous system of size L (with periodic boundary conditions), which corresponds to $N \simeq 40\,000$ atoms. (Solid circles with error bars) System in a circular potential well (see text), with a total atom number $N \simeq 30\,000$ adjusted to have the same central density ρ, hence, the same degeneracy temperature T_d and healing length ξ as in the homogeneous case. The suggested experimental values of Table I correspond to the circled point indicated by the oblique arrow and require the measurement of a relative energy change of $\simeq 0.7\%$. (Thin lines) Quadratic fit (with no linear term; see the text) of the effective f_n as a function of ϵ_{gauge}, over the interval $0.05 \leqslant \epsilon_{\text{gauge}}/(mk_BT_d)^{1/2} < 0.2$ (dashed lines for the spatially homogeneous system and solid lines for the system in the potential well). Black, red, and blue lines and points (from bottom to top) correspond to an excitation sequence with $\gamma/(c_sq) = 0.4, 0.2$, and 0.1, respectively, with $c_s = (\rho g/m)^{1/2}$ the Bogoliubov sound velocity. The extrapolated zero-ϵ_{gauge} values of the effective normal fraction are indicated in the figure. The region between the horizontal dotted lines indicates the confidence interval of the thermodynamic prediction shown in Fig. 3. The residual 14% deviation of f_n from the thermodynamic value (after linear extrapolation to $\gamma = 0$) is a finite $q\xi$ effect (see text).

nonlinear effects set in the effective normal fraction and it becomes less clear how to extrapolate them down to $\epsilon_{\text{gauge}} = 0$.

For the sake of completeness, it is important to note that for the weak gauge-field amplitudes that are required to be in the linear regime, or at least in the regime of the numerically suggested linear dependence of the effective normal fraction with $\epsilon_{\text{gauge}}^2$, the deposited energy ΔE_2 is at most a few percentage points of the total energy of the system, which may be experimentally challenging to measure [47]. This value is,

however, larger than the statistical uncertainty of the energy in the canonical ensemble with $n_{real} = 1000$ realizations. As explained in the Appendix E, such a large number of realizations turned out to be necessary in the small ϵ_{gauge} regime to compensate the fluctuations of the current $\mathbf{j}(t = 0)$ at the initial time. The resulting statistical error for the effective normal fraction is about 2% for the parameters of Table I. In the numerical results of Fig. 4, this issue was circumvented by a simulation trick so $n_{real} = 1000$ is a sufficiently large number of realizations to keep error bars below 2% in the limit $\epsilon_{gauge} \to 0$ [48]. It is also shown in Appendix E that a measurement of the *variance* of the deposited energy (rather than its mean value), in principle, also allows us to access the normal fraction, if one knows experimentally the initial energy of the gas.

After linear extrapolation to $\gamma = 0$ from the lowest two values of γ in Fig. 4, which gives $f_n \simeq 0.176$, the residual disagreement of f_n with the thermodynamic result indicated by the dotted lines is about 14%, of the same order as the finite q correction predicted by Bogoliubov theory; see Fig. 2(a). We have, thus, performed simulations for $q\xi = 1/2$ for a spatially homogeneous system having the same parameters as in Fig. 4 and for a gauge-field switch-off rate $\gamma/(c_s q) = 0.2$ (not shown). It is found that the range of linearity of the effective normal fraction with ϵ_{gauge}^2 is of the same order, up to $\epsilon_{gauge}/(mk_B T_d)^{1/2} \simeq 0.27$. Repeating the zero-$\epsilon_{gauge}$ extrapolation procedure as in Fig. 4, we find for $q\xi = 1/2$ an effective normal fraction of 0.164(3) rather than 0.146(2) for $q\xi = 1$. Assuming a quadratic dependence of the effective normal fraction with q at fixed $\gamma/(c_s q)$, as predicted by Bogoliubov theory, see Fig. 2(b), this leads to an additive correction to f_n close to 0.024. We finally reach $f_n \simeq 0.20$, which is within the statistical error bars of the thermodynamic value [49]. On a smaller system with $M = 32^2$ modes, we have reached a similar conclusion, taking even smaller values of $q\xi$ and $\gamma/(c_s q)$; see the blue circle in Fig. 3 and the figure caption. The deviation observed in Fig. 4 is, therefore, not a systematic error of the proposed method.

As a final check, we have tested the locality of the proposed measurement scheme by performing the simulation for two different geometries. Open squares and dashed lines in Fig. 4 correspond to a spatially homogeneous system with periodic boundary conditions, while the solid disks and solid lines correspond to a system trapped in a circular well with steep walls of the form $U(\mathbf{r}) = \zeta k_B T \{\tanh[(r - L/2)/(\xi/2)] + 1\}$, where the numerical parameter ζ determines the energy cutoff in the classical field model [39]. The probed region is at the center of the potential well, $\mathbf{r}_0 = \mathbf{0}$. Even in the nonlinear regime, where linear response theory fails, the effective normal fractions are almost the same in both geometries.

V. OPTICAL MEASUREMENT

The proposal that we have illustrated in the previous section was based on the measurement of atomic quantities, namely the deposited energy in the atomic cloud at the end of the gauge-field sequence. The present section is devoted to the presentation and the characterization of an alternative, all-optical route to measure the normal fraction f_n: Information on the response of the atomic cloud to the gauge field can
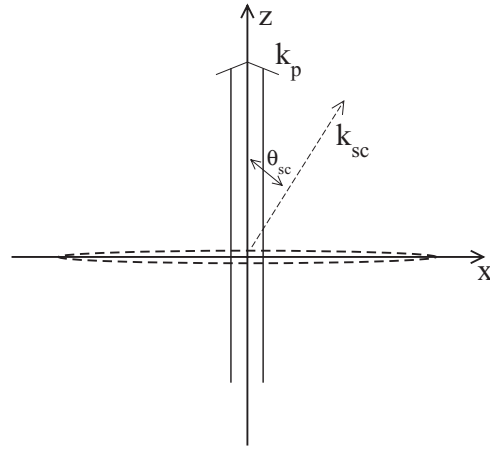

FIG. 5. Scheme of the scattering geometry under examination in Sec. V B. Probe light is incident at wave vector $\mathbf{k}_p = k_p \mathbf{e}_z$ and the scattered light is collected at a wave vector $\mathbf{k}_{sc} = (k_p^2 - Q^2)^{1/2} \mathbf{e}_z + \mathbf{Q}$.

be retrieved from the transmitted probe beams once they have crossed the atomic cloud. Recent works have in fact pointed out that the strong frequency dependence of the dielectric constant of an optically dressed medium in the electromagnetically induced transparency (EIT), already used experimentally to strongly reduce the light group velocity [50–52], can be exploited for velocimetry experiments: Information on the current profile of an atomic cloud was predicted to be imprinted onto the phase of the transmitted probe beam [53,54].

In the present case, the gas is illuminated by probe light of angular frequency ω_p and coupling light of angular frequency ω_c. As in Sec. IV the coupling light is a plane wave propagating along the y axis. In the Sec. V A, where it is proposed to measure the transmitted mean electric field amplitude, the probe light consists, as in Sec. IV, of two beams with wave vectors $\mathbf{k}_p^{\pm}$ at a small angle with the z axis, as shown in Fig. 1; differing from Refs. [53,54], the matter-wave current pattern is generated by the same laser beams that are then used for probing. The configuration differs slightly in Sec. V B, where it is proposed to measure the pattern of the scattered light intensity: In this case, the probe light consists of a single beam with a wave vector $\mathbf{k}_p$ directed along the z axis, as shown in Fig. 5. Even though no spatially modulated matter-wave current is generated by the laser beams, still one can extract information on f_n from the zero-mean matter-wave currents induced by thermal fluctuations in the gas.

A. Extracting f_n from the amplitude of transmitted light

The transmission and reflection of probe light from the two-dimensional atomic cloud can be described in terms of Maxwell equations. In particular, the dipole polarization of the atoms provides a source term for the probe electric field $\mathcal{E}_p$ at angular frequency ω_p: For the positive frequency parts, one has, in the paraxial approximation with respect to the z axis,

$$\left(\Delta + k_p^2\right) \mathcal{E}_p = -\frac{k_p^2}{\epsilon_0} \mathcal{P}_p, \qquad (40)$$

where $k_p = \omega_p/c$ and the Laplacian operator is three dimensional. In the considered Λ atomic configuration, see Fig. 1,

one may think that the atoms occupy in each point of space the noncoupled state $|NC(\mathbf{r})\rangle$, leading to a vanishing mean atomic polarization $\mathcal{P}_p$. This is actually not exactly the case: Due to the atomic motion, the atomic internal state does not follow adiabatically and there exists a small coupling between the position-dependent coupled state $|C(\mathbf{r})\rangle$ and noncoupled state $|NC(\mathbf{r})\rangle$, the so-called motional coupling [28]. This leads to a small nonadiabatic atomic polarization, which we now evaluate.

Within a perturbative picture, we simply need to calculate the mean atomic polarization $\mathcal{P}_p$ induced by the unperturbed laser fields. In terms of the three-dimensional atomic field operators, this reads

$$\mathcal{P}_p(\mathbf{r}) = d_{ae} \langle \hat{\Psi}_a^\dagger(\mathbf{r}) \hat{\Psi}_e(\mathbf{r}) \rangle. \quad (41)$$

With the usual adiabatic elimination of state $|e\rangle$, as shown in Appendix B, the atomic field in the excited state can be written in terms of the atomic field operator $\hat{\chi}_{3D}$ in the coupled $|C\rangle$ state

$$\hat{\chi}_{3D}(\mathbf{r},t) = \langle C(\mathbf{r},t)|a\rangle \hat{\Psi}_a(\mathbf{r},t) + \langle C(\mathbf{r},t)|b\rangle \hat{\Psi}_b(\mathbf{r},t) \quad (42)$$

as

$$\hat{\Psi}_e \simeq \frac{\Omega_c}{2(\delta + i\Gamma/2)} [1 + |\Omega_p/\Omega_c|^2]^{1/2} \hat{\chi}_{3D} + \Gamma^{1/2}\hat{B}_e. \quad (43)$$

From the explicit form of the noise term $\hat{B}_e$ given in Appendix B, it is immediate to see that it gives a zero contribution to the mean in Eq. (41). Since the atoms are mostly in the uncoupled $|NC\rangle$ state, we can approximate the atomic field Ψ_a in the $|a\rangle$ state by its $|NC\rangle$ component. To lowest order in Ω_p/Ω_c we then have

$$\mathcal{P}_p(\mathbf{r}) \simeq \frac{d_{ae}\,\Omega_c}{2(\delta + i\Gamma/2)} \langle \hat{\phi}_{3D}^\dagger(\mathbf{r}) \hat{\chi}_{3D}(\mathbf{r}) \rangle. \quad (44)$$

The next step is to perturbatively evaluate the field $\hat{\chi}_{3D}$ that is created in the coupled $|C\rangle$ state by the motional coupling [28] of $|C\rangle$ to $|NC\rangle$. The details of the procedure are given in the Appendix B. To first order in Ω_p/Ω_c and for the magic choice Eq. (23) of Δ_c, one obtains after adiabatic elimination

$$\hat{\chi}_{3D} \simeq -\frac{4\hbar(\delta + i\Gamma/2)}{m|\Omega_c|^2} \nabla \hat{\phi}_{3D} \cdot \nabla \frac{\Omega_p}{\Omega_c} + \Gamma'^{1/2}\hat{B}_\chi. \quad (45)$$

An explicit expression for the noise term $\hat{B}_\chi$ is given in Appendix B: Again, the noise term has a zero expectation value and does not contribute to the optical polarization. The final form of the optical polarization in terms of the three-dimensional atomic density and current operators (17) and (15) reads, to zeroth order in q/k_p,

$$\mathcal{P}_p(\mathbf{r}) = -\frac{4\,|d_{ae}|^2}{\hbar\,|\Omega_c|^2}(\mathbf{k}_p - \mathbf{k}_c) \cdot \left[\langle \mathbf{j}_{3D}(\mathbf{r}) \rangle + \frac{\hbar}{2im} \nabla\langle n_{3D}(\mathbf{r}) \rangle \right] \\ \times \mathcal{E}_p(\mathbf{r}), \quad (46)$$

where the Rabi frequency of the probe beam has been eliminated in favor of the electric field using the definition $-d_{ea}\mathcal{E}_p = \hbar\Omega_p/2$ and the detuning δ has disappeared from the formula. The first term proportional to the atomic current operator has a simple semi-classical interpretation in terms of the reduced group velocity in the EIT regime, as anticipated in Refs. [53,54]: In this regime, the refractive index strongly

depends on the Raman detuning, which, in turn, depends on the atomic speed because of the Doppler effect.

However, the expression (46) differs from the semiclassical one that was used in Ref. [54] in two ways. First, the current operator in Eq. (46) differs from the physical current of atoms by the gauge field

$$\mathbf{j}_{\text{phys}} = \mathbf{j}_{3D} - \frac{1}{m} n_{3D} \mathbf{A}_{3D}. \quad (47)$$

As the proposal in Ref. [54] addressed a pre-existing current profile and the weak probe beam induced a vanishingly small gauge field, the difference was irrelevant in that case. Here, on the contrary, the mean current is itself proportional to the gauge field so the difference between the two operators really matters. Second, Eq. (46) contains an extra term proportional to the average density gradient. In contrast to the first term, this one is purely imaginary. As a result, it affects only the intensity of the transmitted light *via* a combination of absorption and/or amplification effects. In particular, as it does not induce any phase shift on the light, it does not interfere with the proposal of Ref. [54].

In order to calculate the modification $\delta\mathcal{E}_p$ induced by the atoms on the transmitted electric field of the probe, one has to insert the polarization (46) as a source term into the Maxwell equation (40). Within a standard approximation, we can neglect diffraction effects stemming from the in-plane part of the Laplace operator in Eq. (40) and integrate the z dependence across the atomic cloud. Taking into account the appropriate boundary conditions for $\delta\mathcal{E}_p$, this leads to the expression

$$\delta\mathcal{E}_p(x,y,z) \simeq e^{ik_p z} \frac{ik_p}{2\epsilon_0} \int_{-\infty}^{\infty} dz' \, e^{-ik_p z'} \mathcal{P}_p(x,y,z') \quad (48)$$

for the transmitted field in the $z > 0$ region. In order for the approximation to be accurate, z has to be much larger than the thickness a_{ho}^z of the atomic pancake but, at the same time, much smaller than the diffraction length k_p/q^2, where q is the characteristic wave vector of the in-plane modulation of the atomic density and current.

Along z, the atomic field varies as the harmonic oscillator ground-state wave function $\phi_0(z)$; see Eq. (19). Performing the integral over z', this gives the final expression for the variation of the transmitted field

$$\delta\mathcal{E}_p(\mathbf{r}) = \frac{2ik_p\,|d_{ae}|^2}{\hbar\epsilon_0\,|\Omega_c|^2} \mathbf{k}_c \cdot \left[\langle \mathbf{j}(\mathbf{r}) \rangle + \frac{\hbar}{2im} \nabla\langle n(\mathbf{r}) \rangle \right] \mathcal{E}_p(\mathbf{r}) \quad (49)$$

in terms of the two-dimensional density $n(\mathbf{r})$ and current $\mathbf{j}(\mathbf{r})$ operators. The first contribution proportional to the atomic current gives a phase shift, while the second contribution proportional to the atomic density gradient is responsible for absorption and amplification of the probe beam.

The atomic current profile created by the gauge field is evaluated using the linear response formulas (3) and (4) as discussed in detail in the previous sections. The gauge field is assumed to be switched on slowly enough as compared to the characteristic frequencies of all the excitation modes of the gas at wave vector $\mathbf{q}$. Within the linear response regime, the contribution to the current due to the spatially modulated

gauge field at **q** may be isolated by a suitable combination of measurements with different values of $\Omega_p^\pm$, which gives

$$\langle \mathbf{j} \rangle_2(\mathbf{r}) = \frac{\hbar \rho k_c}{mq |\Omega_c|^2} (\mathbf{q} \cos \alpha + f_n \mathbf{e}_z \times \mathbf{q} \sin \alpha)$$
$$\times (\Omega_p^+ \Omega_p^{-*} e^{i\mathbf{q}\cdot\mathbf{r}} + \Omega_p^{+*} \Omega_p^- e^{-i\mathbf{q}\cdot\mathbf{r}})$$
$$\times e^{-2|\mathbf{r}-\mathbf{r}_0|^2/w^2}, \qquad (50)$$

where **r** is now in the xy plane and α is the oriented angle that $\mathbf{k}_c$ makes with **q** [34]. Inserting this expression into Eq. (49) and recalling the form (7) of the incident probe field, one can extract the phase shift experienced by the central part of the probe beams after crossing the atomic pancake,

$$\Delta\phi_2^\pm = \frac{6\pi\hbar\rho}{m} \frac{|\Omega_p^\mp|^2}{|\Omega_c|^4} B\Gamma [\cos^2\alpha + f_n \sin^2\alpha], \qquad (51)$$

where we have assumed $k_p \simeq k_c$. The total decay rate of the e state by spontaneous emission is indicated by Γ and B is the branching ratio for the decay to the a state, so $B\Gamma = |d_{ae}|^2 k_c^3/(3\pi\hbar\epsilon_0)$. As already mentioned above, the density gradient term in Eq. (49) only introduces an intensity modulation and is not responsible for any phase shift.

From a nonlinear optics point of view, the phase shift (51) can be interpreted as arising from a $\chi^{(3)}$ optical nonlinearity of optomechanical origin similar to the one demonstrated in the experiment [55]: The nonlinear modulation of the optical response of the atoms is determined by the mechanical distortion of the cloud by the optical forces.

Inserting into Eq. (51) the values of Table I for the ^{87}Rb case, for the first choice of level scheme reported in Appendix A, one has a branching ratio $B = 1/4$ and one finds a small, yet appreciable, phase shift on the order of

$$\Delta\phi_2^{\text{choice 1}} \simeq 6 \times 10^{-4} [\cos^2\alpha + f_n \sin^2\alpha]. \qquad (52)$$

For the second choice of level scheme in Appendix A, the branching ratio is slightly larger, $B = 1/3$, but for the compromise choice, Eq. (A25), $|\Omega_c|^2/\Gamma^2$ is larger so one finds a smaller phase shift,

$$\Delta\phi_2^{\text{choice 2}} \simeq 3 \times 10^{-4} [\cos^2\alpha + f_n \sin^2\alpha]. \qquad (53)$$

In addition to the phase shift of the transmitted beam that we have discussed so far, Bragg diffraction on the spatially modulated current profile produces a pair of additional beams of in-plane wave vector, respectively, $\pm 3\mathbf{q}/2$ via a sort-of four-wave mixing process. The relative intensity of these beams as compared to the incident probe beams is on the order of $|\Delta\phi_2|^2$. For transverse gauge fields such that $\mathbf{q} \cdot \mathbf{k}_c = 0$, the contribution of the induced density gradient term of Eq. (49) vanishes by symmetry. In the case of longitudinal gauge fields, the relative correction is on the order of $q\xi$.

B. Current fluctuations and the angular distribution of scattered light

All the calculations presented in the previous subsection aimed at evaluating the expectation value of the transmitted field amplitude. At this level of the theory, we were allowed to describe the probe beam as a coherent, classical field and we could neglect the fluctuations around the expectation value

of both the light field amplitude and the atomic current and density operators. The formalism can be straightforwardly extended to quantum optical fields to include the fluctuations of the atomic density and current. This is crucial when one aims at investigating the spontaneous scattering of light off the current fluctuations in the atomic gas. In this subsection, we shall in particular show how information on the normal fraction of the gas can be inferred from the angular distribution of scattered light. We shall make the approximation of replacing temporal derivatives of the electromagnetic field $\partial_t \mathcal{E}$ by $-ick_p \mathcal{E}$ in Maxwell's equation. In particular, this misses retardation effects in the expression of the scattered fields in terms of the atomic dipoles, which is accurate since the system size is much smaller than c/Γ.

We consider the geometry sketched in Fig. 5: a single Gaussian probe beam is incident onto the atoms with a wave vector $\mathbf{k}_p$ exactly orthogonal to the atomic plane, waist w centered at $\mathbf{r}_0$, and a weak peak amplitude $\mathcal{E}_p^0$. Inserting this form into Eq. (49) and taking the Fourier transform along the xy plane, one obtains the following operator equation for the scattered field component at the in-plane wave vector **Q** [56]:

$$\mathcal{E}(\mathbf{Q},z) \simeq \frac{2i\,k_p\,|d_{ae}|^2}{\epsilon_0\hbar\,|\Omega_c|^2} \pi\,w^2\,\mathcal{E}_p^0 \int \frac{d^2q}{(2\pi)^2} e^{-q^2 w^2/4} e^{-i\mathbf{q}\cdot\mathbf{r}_0}$$
$$\times \left\{ \mathbf{k}_c \cdot \left[\mathbf{j}_{\mathbf{Q}-\mathbf{q}} + \frac{\hbar(\mathbf{Q}-\mathbf{q})}{2m} n_{\mathbf{Q}-\mathbf{q}} \right] \right\} e^{ik_z(\mathbf{Q})z}. \quad (54)$$

Here, $\mathbf{j}_\mathbf{Q}$ and $n_\mathbf{Q}$ are the spatial Fourier transforms of the two-dimensional current $\mathbf{j}(\mathbf{r})$ and density $n(\mathbf{r})$ operators; the Fourier transform of a product of two functions has been rewritten in terms of the convolution of their Fourier transforms. The z component of the propagation wave vector is determined by the photon dispersion as $k_z(\mathbf{Q}) = (k_p^2 - Q^2)^{1/2}$.

The intensity of the scattered light at in the plane wave vector **Q** is quantified by [56]

$$\langle \mathcal{E}^\dagger(\mathbf{Q})\mathcal{E}(\mathbf{Q}) \rangle = \left[\frac{2\pi k_p |d_{ae}|^2 w^2 |\mathcal{E}_p^0|}{\epsilon_0 \hbar |\Omega_c|^2} \right]^2$$
$$\times \int \frac{d^2q}{(2\pi)^2} \int \frac{d^2q'}{(2\pi)^2}$$
$$\times \left\langle \left\{ \mathbf{k}_c \cdot \left[\mathbf{j}_{\mathbf{Q}-\mathbf{q}}^\dagger + \frac{\hbar(\mathbf{Q}-\mathbf{q})}{2m} n_{\mathbf{Q}-\mathbf{q}}^\dagger \right] \right\} \right.$$
$$\times \left. \left\{ \mathbf{k}_c \cdot \left[\mathbf{j}_{\mathbf{Q}-\mathbf{q}'} + \frac{\hbar(\mathbf{Q}-\mathbf{q}')}{2m} n_{\mathbf{Q}-\mathbf{q}'} \right] \right\} \right\rangle$$
$$\times e^{i(\mathbf{q}-\mathbf{q}')\cdot\mathbf{r}_0} e^{-(q^2+q'^2)w^2/4}. \quad (55)$$

Since the system size is much larger than the waist w of the probe beam, we can for simplicity assume an effective translational symmetry along the xy plane. As a consequence, the correlation function that appears in Eq. (55) has a δ-distribution shape around equal wave vectors $\mathbf{Q} - \mathbf{q} = \mathbf{Q} - \mathbf{q}'$ [see, e.g., the next Eq. (56)].

In contrast to the schemes proposed in the previous sections, where the duration $1/\gamma$ of the experiment had to be at least on the order of $1/(c_s q)$, where $c_s = (\rho g/m)^{1/2}$ is the Bogoliubov sound velocity, the light-scattering experiment discussed here can be performed on a much faster time scale, only limited by the characteristic rate Γ' of the internal atomic evolution time,

Eq. (B7). As a result, the experiment can be performed in the small wave-vector region $Q\xi \ll 1$, where the contribution to Eq. (55) of the terms involving the density fluctuations $n_{\mathbf{Q}}$ is negligible [57]. Of course, efficient isolation of the scattered light from the incident beam requires that the scattering angle $\theta_{\rm sc} \simeq Q/k_p$ be much larger than the diffraction cone of the probe beam, i.e., $Q \gg 1/w$.

The instantaneous correlation function of the current in the y direction parallel to $\mathbf{k}_c$ can be evaluated applying the fluctuation-dissipation relation (E5) to the current operator $\mathbf{j}_{\mathbf{q}}$ in an infinite space geometry. This gives

$$
\begin{aligned}
\langle j_{\mathbf{Q},y}^{\dagger} j_{\mathbf{Q}',y} \rangle &= (2\pi)^2 \, \delta^2(\mathbf{Q} - \mathbf{Q}') k_B T \, {\rm Re}[\chi_{yy}(\mathbf{Q}', \omega = 0)] \\
&\underset{Q \to 0}{\simeq} (2\pi)^2 \, \delta^2(\mathbf{Q} - \mathbf{Q}') \frac{k_B T \, \rho(\mathbf{r}_0)}{m} \\
&\quad \times [\cos^2 \phi_{\rm sc} + f_n \sin^2 \phi_{\rm sc}],
\end{aligned}
\tag{56}
$$

where $\phi_{\rm sc}$ is now the azimuthal angle between $\mathbf{k}_c$ and $\mathbf{Q}$. Inserting this expression into Eq. (55) and taking the thermodynamic limit, one gets to the final expression for the scattered intensity in the momentum $\mathbf{Q}$ space [56],

$$
\begin{aligned}
\langle \mathcal{E}_{\mathbf{Q}}^{\dagger} \mathcal{E}_{\mathbf{Q}} \rangle &= \left[\frac{k_p \, k_c \, |d_{ae}|^2}{\epsilon_0 \, \hbar \, |\Omega_c|^2} \right]^2 2\pi w^2 \, |\mathcal{E}_p^0|^2 \frac{k_B T \, \rho(\mathbf{r}_0)}{m} \\
&\quad \times [\cos^2 \phi_{\rm sc} + f_n \sin^2 \phi_{\rm sc}].
\end{aligned}
\tag{57}
$$

To estimate the relative intensity of scattered light, it is useful to rewrite Eq. (57) for the momentum-space intensity $\langle \mathcal{E}_{\mathbf{Q}}^{\dagger} \mathcal{E}_{\mathbf{Q}} \rangle$ in terms of physically more transparent quantities such as the angular distribution $I(\theta_{\rm sc}, \phi_{\rm sc})$ of scattered intensity. For small scattering angles $|\theta_{\rm sc}| \ll 1$, the infinitesimal solid angle and momentum-space volume elements are related by $d\Omega = \sin \theta_{\rm sc} \, d\theta_{\rm sc} \, d\phi_{\rm sc} \simeq \theta_{\rm sc} \, d\theta_{\rm sc} \, d\phi_{\rm sc} \simeq d^2 Q / k_p^2$, so

$$
I_{\rm sc}(\theta_{\rm sc}, \phi_{\rm sc}) \simeq \frac{k_p^2}{(2\pi)^2} \langle \mathcal{E}_{\mathbf{Q}}^{\dagger} \mathcal{E}_{\mathbf{Q}} \rangle.
\tag{58}
$$

This immediately leads to the final expression for the angular distribution of the scattering intensity [56]

$$
\begin{aligned}
\frac{I_{\rm sc}(\theta_{\rm sc}, \phi_{\rm sc})}{I_{\rm inc}} &= \left[\frac{k_p^2 \, k_c \, |d_{ae}|^2}{\pi \, \epsilon_0 \, \hbar \, |\Omega_c|^2} \right]^2 \frac{k_B T \rho(\mathbf{r}_0)}{m} \\
&\quad \times [\cos^2 \phi_{\rm sc} + f_n \sin^2 \phi_{\rm sc}]
\end{aligned}
\tag{59}
$$

in units of the incident intensity,

$$
I_{\rm inc} = \int d^2 r \, |\mathcal{E}_p(\mathbf{r})|^2 = \frac{\pi w^2}{2} |\mathcal{E}_p^0|^2.
\tag{60}
$$

From this expression, it is immediately evident that information on the normal fraction of the gas can be retrieved from the azimuthal dependence of the scattered intensity. In terms of the total spontaneous emission decay rate Γ of the e state and the $|e\rangle \to |a\rangle$ branching ratio B [we recall that $B\Gamma = |d_{ae}|^2 k_c^3 / (3\pi \hbar \epsilon_0)$], Eq. (59) can be rewritten in the more transparent form [56],

$$
\frac{I_{\rm sc}(\theta_{\rm sc}, \phi_{\rm sc})}{I_{\rm inc}} = \frac{9 k_B^2 T \, T_d}{2\pi \hbar^2} \frac{B^2 \Gamma^2}{|\Omega_c|^4} [\cos^2 \phi_{\rm sc} + f_n \sin^2 \phi_{\rm sc}].
\tag{61}
$$

To estimate the feasibility of the proposed light scattering experiment, we now derive an upper bound on the number

of useful scattered photons in a single shot of duration τ. Calculating the Poynting's vector of the probe beam, and using Eq. (60), we find an incident flux of probe photons $\Phi_{\rm inc} = (k_p w)^2 |\Omega_p^0|^2 / (12 B \Gamma)$. Integrating in Eq. (59) the term proportional to f_n over solid angles in the cone $\theta_{\rm sc} \leqslant 1/(k_p \xi)$, we obtain the flux $\Phi_{\rm sc}^{\rm use}$ of useful scattered photons. As a maximal duration, we take $\tau = 1/\Gamma_{\rm fluo}^{\rm non-ad}$, where the fluorescence rate of the atoms due to motional coupling between the noncoupled and the coupled states is given by Eq. (A2) (with $2|\Omega_p^+|^2$ replaced here with $|\Omega_p^0|^2$). The number of single shot useful scattered photons is, thus, bounded by

$$
N_{\rm ph}^{\rm use} \leqslant \frac{3\pi B}{16} \frac{k_B T}{\hbar \omega_z} \rho w^2 f_n \frac{1}{(k_c \xi)^2}.
\tag{62}
$$

Remarkably, the Rabi frequencies Ω_c and Ω_p^0 have canceled out in the ratio of the scattered flux to the fluorescence rate. One recognizes in the right-hand side of expression (62) the effective mean number of atoms $N_{\rm at}^{\rm eff} = \pi \rho w^2 f_n / 4$ in the normal component illuminated by the probe beam, as in Eq. (28). There is, however, a severe geometrical reduction factor, $1/(k_c \xi)^2$, due to the small aperture of the useful scattering cone. For the parameters of Table I, with $B = 1/3$, and taking a waist $w = 30\xi$ and $f_n = 0.2$ as in Fig. 4, we find $N_{\rm at}^{\rm eff} \simeq 1400$, $1/(k_c \xi) \simeq 0.15$, which leads to $N_{\rm ph}^{\rm use} \leqslant 5$. This remains accessible to current quantum optics experiments. For fixed $k_B T / \hbar \omega_z$, the upper bound in Eq. (62) scales as ρ^2, since $1/\xi^2$ scales as ρ, so larger values of photon numbers for a given waist may be obtained by increasing the density ρ of the two-dimensional Bose gas.

VI. CONCLUSIONS AND PERSPECTIVES

In this article we have proposed and validated two methods to measure the superfluid fraction of a quantum fluid of ultracold atoms. The idea is to apply an artificial gauge field to the atoms with spatial oscillations within a localized envelope and to detect, within the linear response regime, the matter-wave current pattern that is generated in the fluid. This can be done in a mechanical way by measuring the energy that is deposited in the fluid at the end of a gauge-field sequence. This can also be done in an all-optical way by observing the phase shift experienced by the same laser beams that are used to generate the artificial gauge field or the angular pattern of scattered light. We have shown that, by a careful choice of the parameters and of the atomic level scheme for ^{87}Rb, two experimental obstacles, the spontaneous emission and (in the case of the mechanical method) undesired light shifts, can be put to an acceptable level. The experimental challenge remains in the required high sensitivity of the measurements, that is, a detection of small energy changes in the mechanical method, and a detection of small optical phase shifts or small photon numbers in the all-optical methods.

The interest of the proposed methods is twofold: They do not require that the gas reaches thermal equilibrium in presence of the gauge field, and, furthermore, they give the possibility of reconstructing in a local way the spatial profile of the superfluid fraction of a trapped gas, independently from the presence or the absence of a Bose-Einstein condensate. This last feature is attractive in the study of the Berezinskii-Kosterlitz-Thouless transition to a superfluid state in two-dimensional Bose gases
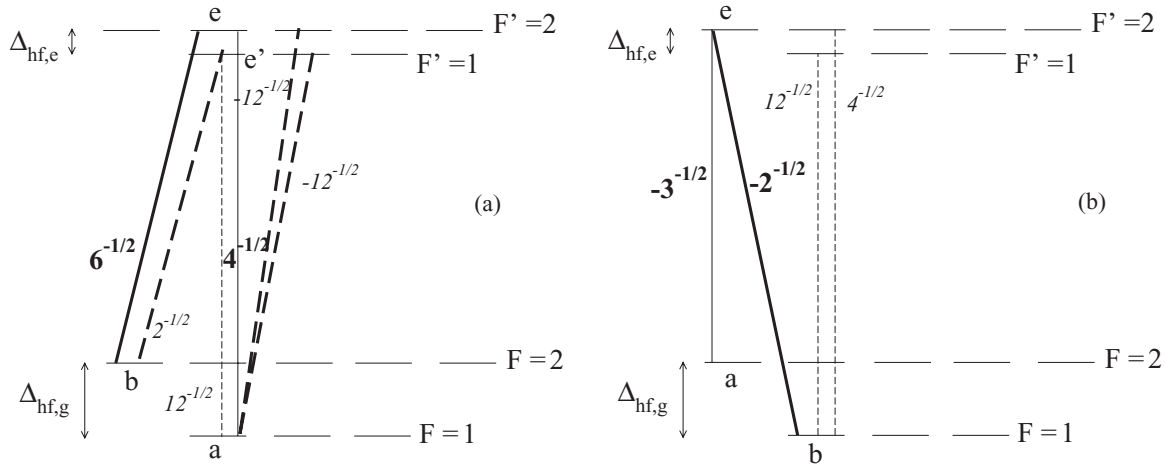
FIG. 6. Scheme of the internal levels of ^{87}Rb atom involved in the D_1 transition ($J = 1/2 \rightarrow J' = 1/2$). The hyperfine splitting of the ground (excited) state is $\Delta_{\mathrm{hf},g} = 2\pi 6.834$ GHz ($\Delta_{\mathrm{hf},e} = 2\pi 814$ MHz). The natural linewidth of the excited state is $\Gamma = 2\pi 5.75$ MHz. Thin (thick) lines indicate transitions that are induced by the probe (coupling) beams. Solid (dashed) lines indicate the desired (main undesired) transitions. The relevant dipole matrix elements are shown in units of the reduced dipole element $\langle J = 1/2 || er || J' = 1/2 \rangle$ of the D_1 line, in bold for the desired transitions and in italic for the undesired ones. Our first choice for the Λ system $|a\rangle, |e\rangle, |b\rangle$ states is shown, in the left (a) panel, with $|a\rangle = |F = 1, m_F = -1\rangle$, $|e\rangle = |F' = 2, m_{F'} = -1\rangle$, $|b\rangle = |F = 2, m_F = -2\rangle$. The second choice is shown in the right (b) panel, with $|a\rangle = |F = 2, m_F = -2\rangle$, $|e\rangle = |F' = 2, m_{F'} = -2\rangle$, $|b\rangle = |F = 1, m_F = -1\rangle$. Note that we have taken the y axis as the quantization axis of angular momenta.

and of the superfluidity properties of Bose gases in disordered environments. It would also be interesting to extend the method to the study of superfluidity in multicomponent atomic fermionic gases, which may require identification of suitable level schemes.

APPENDIX A: EXPERIMENTAL ISSUES

In this Appendix we review some issues that may hinder an experimental implementation of our proposal. Our attention will be concentrated onto the most relevant case of ^{87}Rb atoms considered in the experiment of Refs. [58,59] and, in a two-dimensional context, in Ref. [4]. The level structure of this atomic species is sketched in Fig. 6. A possibly important advantage of this atom in view of an experimental implementation of the present proposal is that the singlet and triplet scattering lengths of ground-state atoms are equal within a few percentage points [60]. We, thus, expect that all scattering lengths between arbitrary $F = 1$ or $F = 2$ sublevels of the ground state have all almost the same values [61], which leads to $g_{aa} \simeq g_{ab}$ and, therefore, to a suppression of the spatiotemporal variation of the effective interaction constant $g_{3D}(\mathbf{r},t)$ defined in Eq. (18). In the deposited energy method proposed in Sec. IV, this is important to reduce the emission of phonons in the atomic gas by the temporal

modulation of the interaction constant. In the optical detection scheme of Sec. V, this is also important to suppress the contribution of the interaction term to the field $\hat{\chi}_{3D}$ and then to the optical polarization. Other atomic species such as Yb [17] or metastable He [62,63] and/or different laser beam configurations [18,19,64] are expected to be useful for other purposes, e.g., to suppress spontaneous emission and/or generate artificial gauge fields with different geometries [65].

Two possible choices for the three states $|a\rangle, |b\rangle, |e\rangle$ forming the Λ system on the $D1$ line of ^{87}Rb are considered, as shown in Figs. 6(a) and 6(b). For each choice, we determine the undesired effects (spontaneous emission, light shifts, Raman leaks) stemming from deviations from the perfect adiabatic following of the noncoupled state by the moving atoms and from optical transitions to other levels not included in the Λ system. An eye will also be kept on trying to maximize the $|e\rangle$ to $|a\rangle$ branching ratio to reinforce the optical signal of Sec. V. To minimize spontaneous emission within the low saturation regime, we shall allow for a small detuning δ of both the probe and coupling beam carrier frequencies from the $|a\rangle \rightarrow |e\rangle$ and $|b\rangle \rightarrow |e\rangle$ transitions, respectively. The Raman detuning of the two beams is taken in a way to always fulfill the magic Raman condition (23).

1. First choice

The coupling beam propagates along the y axis and is taken with a σ_+ polarization with respect to the y quantization axis. The probe beam is taken as linearly polarized along y. For the three atomic levels forming the Λ system, we take $|a\rangle \equiv |F = 1, m_F = -1\rangle$, $|b\rangle \equiv |F = 2, m_F = -2\rangle$, and $|e\rangle \equiv |F' = 2, m_{F'} = -1\rangle$ [68]. This scheme of levels and lasers is illustrated in Fig. 6(a). To estimate the importance of the nonadiabatic coupling between the $|\mathrm{NC}\rangle$ and the $|\mathrm{C}\rangle$ states due to the atomic motion, we can evaluate the ratio

ρ_C/ρ_{NC} of the two-dimensional densities in the two states close to the center of the laser spot. This is done using the explicit formula (45) for the field in the $|C\rangle$ state [69]. Using the fact that for quasi-2D samples the gradient is mostly along the harmonically trapped z direction and assuming $\Omega_p^+ = \Omega_p^-$, we obtain for $k_p \simeq k_c$:

$$\frac{\rho_C}{\rho_{NC}} \simeq \left| \frac{4(\delta + i\Gamma/2)k_c\,\Omega_p^+}{\Omega_c^3} \right|^2 \frac{\hbar\omega_z}{m}. \quad (A1)$$

Accuracy of the adiabatic approximation requires that this ratio is much smaller than unity.

The finite population that is present in the $|C\rangle$ state as a consequence of nonperfect adiabaticity is responsible for the spontaneous emission of photons at a single atom rate:

$$\Gamma_{\text{fluo}}^{\text{non-ad}} = \Gamma' \frac{\rho_{NC}}{\rho_C} = 4\Gamma \frac{|\Omega_p^+|^2}{|\Omega_c|^4} \frac{\hbar k_c^2}{m} \omega_z, \quad (A2)$$

where the fluorescence rate Γ' of the coupled state $|C\rangle$ is defined by Eq. (11) and a spatial average has been performed. Remarkably, $\Gamma_{\text{fluo}}^{\text{non-ad}}$ does not depend on the detuning δ.

Other contributions to the fluorescence rate come from nonresonant excitation processes. Dominating among these are the excitation of the $|a\rangle$ state to the states $|F' = 1$ or $2, m_{F'} = 0\rangle$ by the coupling beam at a rate

$$\Gamma_{\text{fluo}}^c = \Gamma \frac{|\Omega_c|^2}{4\Delta_{\text{hf},g}^2}, \quad (A3)$$

and the excitation of the noncoupled state $|NC\rangle$ to $|e'\rangle = |F' = 1, m_{F'} = -1\rangle$ by the total probe plus coupling field with an effective Rabi frequency $-2\Omega_p/\sqrt{3}$, which results in the fluorescence rate on the parasitic Λ' configuration $|a\rangle \rightarrow |e'\rangle \rightarrow |b\rangle$:

$$\Gamma_{\text{fluo}}^{\Lambda'} = \frac{2}{3}\Gamma \frac{|\Omega_p^+|^2}{\Delta_{\text{hf},e}^2}. \quad (A4)$$

In these expressions, we have taken into account the tabulated hyperfine dipole matrix elements of the various optical transitions, and we have introduced the hyperfine splittings $\Delta_{\text{hf},g}$ and $\Delta_{\text{hf},e}$ given for ^{87}Rb in the caption of Fig. 6. Limiting ourselves to the most relevant regime where $|\Omega_p^+/\Omega_c|^2 > 1/100$, we see that in the present case of ^{87}Rb atoms, $\Gamma_{\text{fluo}}^{\Lambda'} \gg \Gamma_{\text{fluo}}^c$.

The total fluorescence rate can then be approximated as the sum of $\Gamma_{\text{fluo}}^{\Lambda'}$ and $\Gamma_{\text{fluo}}^{\text{non-ad}}$. For a given value of the gauge field (proportional to $|\Omega_p^+/\Omega_c|^2$), the total fluorescence rate is minimized to

$$\Gamma_{\text{fluo}}^{\min} \simeq \frac{4\sqrt{6}}{3} \left| \frac{\Omega_p^+}{\Omega_c} \right|^2 \frac{\Gamma}{\Delta_{\text{hf},e}} \left(\frac{\hbar k_c^2 \omega_z}{m} \right)^{1/2} \quad (A5)$$

by a careful choice of the coupling beam Rabi frequency

$$\left| \Omega_c^{\text{opt}} \right|^2 = \Delta_{\text{hf},e} \sqrt{\frac{6\hbar k_c^2 \omega_z}{m}} = \frac{\sqrt{3}\Delta_{\text{hf},e}}{2\pi^{1/2}} \frac{\hbar k_c}{m a_{3D}} \tilde{g}. \quad (A6)$$

Here, we have expressed ω_z in terms of the three-dimensional scattering length a_{3D} and the reduced two-dimensional coupling constant as given by Table I and Eq. (20). Inserting the actual parameters of the ^{87}Rb atom, and taking $\tilde{g} = 0.1$, we obtain $|\Omega_c^{\text{opt}}|^2/\Gamma^2 \simeq 0.21$. It remains to adjust the detuning δ

to be in the weak saturation regime,

$$s \equiv \frac{|\Omega_c|^2/2}{|\delta + i\Gamma/2|^2} \lesssim \frac{1}{10}. \quad (A7)$$

Let us take the same values of the gauge-field sequence as in Fig. 4: $\gamma/(c_s q) = 0.2$ and $q\xi = 1$ and $\epsilon_{\text{gauge}} \simeq 0.15(m k_B T_d)^{1/2}$, $c_s = (\rho g/m)^{1/2}$ being the Bogoliubov sound velocity. This choice of ϵ_{gauge} leads to $|\Omega_p^+(0^+)/\Omega_c|^2 \simeq 0.03(\rho\lambda_c^2)^{1/2}$: As this quantity has to be much smaller than 1 in order for the gauge-field description of Sec. III to be valid, it is safe to impose $\rho\lambda_c^2 < 10$. Integrating over the exponential switch-off ramp of Ω_p and eliminating g in terms of ω_z and a_{3D}, this gives for the total fluorescence probability per atom,

$$P_{\text{fluo}} = \frac{\sqrt{6}}{2} \frac{\Gamma}{\Delta_{\text{hf},e}} \left(\frac{k_B T_d \hbar\omega_z}{\rho^2 g^2} \right)^{1/2} = \frac{\sqrt{6}}{4} \frac{\Gamma}{\Delta_{\text{hf},e}} \frac{1}{(\rho a_{3D}^2)^{1/2}}. \quad (A8)$$

For ^{87}Rb with the choice $\rho\lambda_c^2 = 9$, we obtain the following result, which is not very impressive:

$$P_{\text{fluo}} \simeq 0.22. \quad (A9)$$

For the sake of completeness, it is important to note that for this choice, $k_B T = 0.1 k_B T_d$ remains smaller than $\hbar\omega_z$, so the Bose gas retains a two-dimensional character.

The existence of other atomic levels in addition to the ones strictly needed to create the gauge field not only is responsible for dissipative effects, such as fluorescence, but also creates reactive effects such as a spatially and temporally dependent light shift of the noncoupled state $|NC\rangle$. Among the dominating processes, the parasitic Λ' scheme creates a modulated light-shift potential

$$U^{\Lambda'}(\mathbf{r}) = \frac{\hbar\,|\Omega_p(\mathbf{r})|^2}{3\Delta_{\text{hf},e}}. \quad (A10)$$

A shift of the same order of magnitude arises from the coupling of the $|a\rangle$ state to the $|F' = 2$ or $1, m_{F'} = 0\rangle$ by the coupling beam.

An estimate of the energy deposited in the system by the $U^{\Lambda'}$ term as compared to the one ΔE_2 due to the gauge field can be obtained with Bogoliubov theory: Using Eq. (D15) with $\mathcal{U}_0 = \hbar(\Omega_p^+\Omega_p^{-*})(0^+)/(3\Delta_{\text{hf},e})$, $\eta = \gamma$, and $\mathbf{Q} = \mathbf{q}$, one gets for $\hbar\gamma \ll \epsilon_q \ll \rho g$:

$$\frac{\Delta E_{U^{\Lambda'}}}{\Delta E_2} = \frac{|\Omega_c|^4}{9 f_n (k_c c_s)^2 \Delta_{\text{hf},e}^2}. \quad (A11)$$

For actual parameters, the energy change due to $\Delta U^{\Lambda'}$ turns out to be non-negligible. For the optimal value of the Rabi frequency Ω_c^{opt} from Eq. (A6), the ratio is

$$\frac{\Delta E_{U^{\Lambda'}}}{\Delta E_2} = \frac{2\hbar\omega_z}{3 f_n \rho g}. \quad (A12)$$

For ^{87}Rb, one finds the discouraging result $\Delta E_{U^{\Lambda'}}/\Delta E_2 \simeq 600\tilde{g}/(\rho\lambda_c^2 f_n)$, which remains much larger than unity even for $\rho\lambda_c^2 = 9$.

Even if the deposited energy by the spurious potential $U^{\Lambda'}$ is much larger than the desired one of the gauge field, a suitable extrapolation procedure may take advantage of the different dependence on the laser intensities to isolate the effect of the

gauge potential. An alternative possibility is to exploit the fact that the $\Delta E_{U^{\Lambda'}}$ contribution does not depend on the direction of $\mathbf{q}$: Within the regime of linear response, this contribution can, therefore, be eliminated by taking the difference of the energy changes for, respectively, longitudinal and transverse gauge fields.

Another possible nuisance is the existence of stimulated Raman processes that may outcouple the noncoupled $|NC\rangle$ state to atomic ground state sublevels $|c\rangle$ other than $|a\rangle$ and $|b\rangle$, via excited state sublevels other than $|e\rangle$ [70]. One may, however, check that, for the proposed scheme, these leaky Raman couplings are detuned from resonance by a frequency amount at least $\Delta_{\mathrm{hf},g}$ in absolute value and, therefore, harmless.

2. Second choice

Another possible choice for ^{87}Rb atoms is to take a σ_- polarization for the coupling beam propagating along the y axis. The probe beam is, again, linearly polarized along y. The atomic levels forming the Λ system are now $|a\rangle \equiv |F = 2, m_F = -2\rangle$, $|b\rangle \equiv |F = 1, m_F = -1\rangle$, and $|e\rangle \equiv |F' = 2, m_{F'} = -2\rangle$. The strong two-body losses that are generally experienced by the upper hyperfine manifold of the ground state are here suppressed by the choice of a maximal m_F state for $|a\rangle$: as collisions between ultracold atoms mostly occur in the s-wave scattering channel, conservation of the sum of the m_F's then prevents transition to the lower hyperfine manifold.

The fluorescence rate per atom due to the motional coupling between $|NC\rangle$ and $|C\rangle$ is still given by $\Gamma_{\mathrm{fluo}}^{\mathrm{non-ad}}$ as defined in Eq. (A2). As there is no longer any parasitic Λ' system, the fluorescence due to laser excitation of $|a\rangle$ or $|b\rangle$ to excited state sublevels other than $|e\rangle$ is now dominated by the transitions $|b\rangle \rightarrow |F' = 1$ or $2, m_{F'} = -1\rangle$ due to the probe beam. Thanks to the reduced occupation probability $\simeq |\Omega_p|^2/|\Omega_c|^2$ of sublevel $|b\rangle$ in the atomic state $|NC\rangle$ and to the larger hyperfine splitting $\Delta_{\mathrm{hf},g}$ of the ground state, the fluorescence rate is strongly suppressed. After spatial averaging it amounts to

$$\Gamma_{\mathrm{fluo}}^p = \frac{3}{2}\Gamma \frac{|\Omega_p^+|^4}{\Delta_{\mathrm{hf},g}^2 |\Omega_c|^2}. \tag{A13}$$

Other fluorescence processes on the D_2 line (e.g., the transition $|a\rangle \rightarrow |J' = 3/2, F' = 3, m_{F'} = -3\rangle$ excited by the coupling beam) are several orders of magnitude weaker than Γ_{fluo}^p thanks to the huge fine structure splitting of $2\pi\, 7$ THz.

Since the two terms in the sum $\Gamma_{\mathrm{fluo}}^{\mathrm{non-ad}} + \Gamma_{\mathrm{fluo}}^p$ experience different switch-off functions $e^{-\gamma t}$ and $e^{-2\gamma t}$, we integrate over time to calculate the total fluorescence probability:

$$P_{\mathrm{fluo}} = \frac{4\Gamma}{\gamma} \frac{|\Omega_p^+(0^+)|^2}{|\Omega_c|^4} \frac{\hbar k_c^2}{m}\omega_z + \frac{3\Gamma}{4\gamma} \frac{|\Omega_p^+(0^+)|^4}{|\Omega_c|^2 \Delta_{\mathrm{hf},g}^2}. \tag{A14}$$

After optimization over the coupling beam intensity, the minimal fluorescence probability

$$P_{\mathrm{fluo}}^{\min} = \frac{2\sqrt{3}}{\gamma} \frac{\Gamma}{\Delta_{\mathrm{hf},g}} \left| \frac{\Omega_p^+(0^+)}{\Omega_c} \right|^3 \left(\frac{\hbar k_c^2}{m}\omega_z \right)^{1/2} \tag{A15}$$

is obtained for a coupling beam Rabi frequency such that

$$|\Omega_c^{\mathrm{opt}}|^4 = \frac{16}{3} \frac{|\Omega_c|^2}{|\Omega_p^+|^2} \Delta_{\mathrm{hf},g}^2 \frac{\hbar k_c^2}{m}\omega_z. \tag{A16}$$

Introducing the reduced quantities $\tilde{\gamma} = \hbar\gamma/(\rho g)$ and $\tilde{\epsilon}_{\mathrm{gauge}} = \epsilon_{\mathrm{gauge}}/(m k_B T_d)^{1/2}$, and eliminating ω_z in terms of g and a_{3D}, we, finally, obtain

$$P_{\mathrm{fluo}}^{\min} = \left(\frac{9}{128\pi} \right)^{1/4} \frac{\tilde{\epsilon}_{\mathrm{gauge}}^{3/2}}{\tilde{\gamma}} \frac{\Gamma}{\Delta_{\mathrm{hf},g}} \frac{\lambda_c}{a_{3D}} (\rho\lambda_c^2)^{-1/4}. \tag{A17}$$

For the parameters of Table I, in particular $\rho\lambda_c^2 = 9$, one finds $|\Omega_c^{\mathrm{opt}}|^2/\Gamma^2 \simeq 5.5$ so a detuning $|\delta| > 5\Gamma$ is required to remain in the weak saturation regime. This resulting probability of spontaneous emission per atom in the deposited energy measurement is very small,

$$P_{\mathrm{fluo}} \simeq 0.008. \tag{A18}$$

As compared to the first one, this second choice then provides a strong reduction of the spontaneous emission rate by a factor of almost 30.

Another advantage of this second choice is that light-shift effects are potentially smaller thanks to the absence of the parasitic Λ' scheme. The probe beam on the $|b\rangle \rightarrow |F' = 1$ or $2, m_{F'} = -1\rangle$ transitions produces a light shift which, after averaging in the $|NC\rangle$ state, leads to the spurious potential

$$U^p(\mathbf{r}) = -\frac{\hbar|\Omega_p|^4}{4|\Omega_c|^2 \Delta_{\mathrm{hf},g}}. \tag{A19}$$

The amount of energy that is deposited in the gas by this spurious potential can be estimated using Eq. (D15) twice, first with $\mathcal{U}_0 = -\hbar|\Omega_p^+(t = 0^+)|^4/(|\Omega_c|^2 \Delta_{\mathrm{hf},g})$, $\eta = 2\gamma$, $\mathbf{Q} = \mathbf{q}$, and second with $\mathcal{U}_0$ four times smaller, $\eta = 2\gamma$, $\mathbf{Q} = 2\mathbf{q}$. Neglecting $2\hbar\gamma$ with respect to ϵ_q, and taking $q\xi = 1$, we obtain the following estimate for the spurious deposited energy:

$$\Delta E_{U^p} = \frac{133}{160} \frac{N}{\rho g} \frac{\hbar^2 |\Omega_p^+(0^+)|^8}{|\Omega_c|^4 \Delta_{\mathrm{hf},g}^2}. \tag{A20}$$

For the coupling beam Rabi frequency (A16) minimizing spontaneous emission, the ratio of the energies deposited by the gauge field and the spurious potential amounts to

$$\frac{\Delta E_{U^p}}{\Delta E_2} = \frac{133\sqrt{2}}{960\pi^{3/2}} \frac{\tilde{g}\,\tilde{\epsilon}_{\mathrm{gauge}}}{f_n} \frac{\lambda_c}{\rho^{1/2} a_{3D}^2}. \tag{A21}$$

For $\tilde{g} = 0.1$ and $\tilde{\epsilon}_{\mathrm{gauge}} = 0.15$ and using the ^{87}Rb parameters summarized in Table I, one finds the still quite unfortunate result

$$\frac{\Delta E_{U^p}}{\Delta E_2} \simeq \frac{4}{f_n} \gg 1. \tag{A22}$$

A possibility to overcome this difficulty and separate ΔE_2 from ΔU^p is to use the same strategy proposed to separate ΔE_2 from ΔE_1 by exploiting the different dependence of the two quantities on the ratio $|\Omega_p^+/\Omega_p^-|(0^+)$. This can be combined with the choice of a compromise value of $|\Omega_c|^2/\Gamma^2$ that allows us to strongly suppress the light-shift potential without introducing a too-large spontaneous emission rate.

To this purpose, we fix $\tilde{\epsilon}_{\text{gauge}} = 0.15$, $\gamma = 0.2\rho g/\hbar$, $q\xi = 1$, $\tilde{g} = 0.1$ and we take as free parameters $X = \rho\lambda_c^2$ and $Y = |\Omega_c|^2/\Gamma^2$. Inserting the relevant parameters for ^{87}Rb as in Table I, we obtain

$$P_{\text{fluo}} = \frac{6.86 \times 10^{-2}}{X^{1/2}Y} + 7.46 \times 10^{-4}Y, \qquad (A23)$$

$$\frac{\Delta E_{U^P}}{\Delta E_2} = \frac{0.132Y^2}{f_n}. \qquad (A24)$$

A reasonable compromise between the two competing effects is to choose $X = 9$ and $Y = 0.5$, which corresponds to

$$\rho\lambda_c^2 = 9 \quad \text{and} \quad \frac{|\Omega_c|^2}{\Gamma^2} = 0.5. \qquad (A25)$$

As a result, for the same parameters $T/T_d = 0.1$ and $f_n = 0.2$ used in the classical field simulations of Sec. IV, we obtain the quite encouraging values

$$P_{\text{fluo}} \simeq 0.045 \qquad (A26)$$

$$\frac{\Delta E_{U^P}}{\Delta E_2} \simeq 0.16. \qquad (A27)$$

We have checked that at the resulting temperature $k_B T/\hbar\omega_z = 0.62$ the Bose gas retains a two-dimensional character and that the validity of the gauge field model of Sec. III is guaranteed by the resulting probe beam Rabi frequency $|\Omega_p^+(0^+)|^2/|\Omega_c|^2 = 0.03X^{1/2} = 0.09 \ll 1$.

To conclude, we remark that the energy deposited by the spurious light shift is suppressed in the extrapolation procedure proposed in Sec. IV C to eliminate effects beyond the linear response regime to the gauge field, that is, an extrapolation of the effective normal fraction that is linear in $\epsilon_{\text{gauge}}^2$. Since ΔE_{U^P} scales as $|\Omega_p^+(0^+)|^8$ with the probe beam Rabi frequency, it varies as $\epsilon_{\text{gauge}}^4$ with the amplitude of the gauge field, so it indeed contributes to the effective normal fraction as $\epsilon_{\text{gauge}}^2$, which extrapolates to zero. This works, of course, for ϵ_{gauge} small enough for the mechanical effect of the spurious light shift to be treatable in the linear response regime.

APPENDIX B: DUM-OLSHANII THEORY FOR MANY-BODY SYSTEMS

In a seminal work [16], Dum and Olshanii have shown that an effective gauge field appears in the theoretical description of a three-level atom interacting with a laser field on a Λ transition. Here we use the formalism of the quantum stochastic differential equations (see, e.g., §8.3.2 of Ref. [30]) to extend this idea to an interacting Bose gas in second quantized form.

We start with the master equation for the density operator $\hat{\sigma}$ of the many-body system, assuming for simplicity that spontaneous emission corresponds to a net loss of atoms,

$$\frac{d}{dt}\hat{\sigma} = \frac{1}{i\hbar}[H,\hat{\sigma}] + \Gamma \int d^3r \left[\hat{\Psi}_e(\mathbf{r})\hat{\sigma}\hat{\Psi}_e^\dagger(\mathbf{r}) \right.$$
$$\left. - \frac{1}{2}\{\hat{\Psi}_e^\dagger(\mathbf{r})\hat{\Psi}_e(\mathbf{r}),\hat{\sigma}\} \right], \qquad (B1)$$

where [,] ({,}) stands for the commutator (anticommutator). The Hamiltonian H is the sum of the single-particle kinetic

and trapping terms, of the interaction terms (that we formally model as local Dirac δ interactions), of the internal energy of the atomic excited state, and of the coupling terms of the atoms to the laser fields.

Since the loss rate $\hbar\Gamma$ greatly exceeds the kinetic, trapping, and interaction energies, we can neglect the external dynamics of the excited state and write

$$H \simeq \int d^3r \sum_{\alpha=a,b} \left[-\frac{\hbar^2}{2m}\hat{\Psi}_\alpha^\dagger \Delta \hat{\Psi}_\alpha + U_{3D}\hat{\Psi}_\alpha^\dagger \hat{\Psi}_\alpha \right]$$
$$+ \int d^3r \left[\frac{g_{aa}}{2}\hat{\Psi}_a^{\dagger 2}\hat{\Psi}_a^2 + \frac{g_{bb}}{2}\hat{\Psi}_b^{\dagger 2}\hat{\Psi}_b^2 + g_{ab}\hat{\Psi}_a^\dagger\hat{\Psi}_b^\dagger\hat{\Psi}_b\hat{\Psi}_a \right]$$
$$+ \int d^3r \, (-\hbar\delta)\hat{\Psi}_e^\dagger\hat{\Psi}_e$$
$$+ \int d^3r \left[\frac{\hbar\Omega_p}{2}\hat{\Psi}_e^\dagger\hat{\Psi}_a + \frac{\hbar\Omega_c}{2}\hat{\Psi}_e^\dagger\hat{\Psi}_b + \text{H.c.} \right]. \qquad (B2)$$

As previously defined, δ is the common value of the detuning of the probe and coupling beams from the $|a\rangle \rightarrow |e\rangle$ and $|b\rangle \rightarrow |e\rangle$ transitions.

In a Heisenberg picture for the open atomic system, the ground-state atomic field operators $\hat{\Psi}_{\alpha=a,b}$ satisfy the usual evolution equations $i\hbar\partial_t\hat{\Psi}_\alpha = [\hat{\Psi}_\alpha, H]$. On the other hand, conservation of the canonical commutation relations of the fields and of the Hermitian conjugation relation between $\hat{\Psi}_\alpha$ and $\hat{\Psi}_\alpha^\dagger$ requires including a quantum Langevin term $\hat{F}_e$ in the evolution equation for the excited state field $\hat{\Psi}_e$,

$$\partial_t\hat{\Psi}_e = \frac{1}{i\hbar}[\hat{\Psi}_e, H] - \frac{1}{2}\Gamma\hat{\Psi}_e + \Gamma^{1/2}\hat{F}_e(\mathbf{r},t). \qquad (B3)$$

Here, the quantum noise term $\hat{F}_e$ is δ correlated in position and time, e.g., $[\hat{F}_e(\mathbf{r},t), \hat{F}_e^\dagger(\mathbf{r}',t')] = \delta(\mathbf{r}-\mathbf{r}')\delta(t-t')$, and we recall that the expectation value of normally ordered products of noise operators vanish, e.g., $\langle\hat{F}_e^\dagger\hat{F}_e\rangle = 0$, since the bath does not provide an incoming flux of e atoms.

The only nonzero contributions to the commutator in Eq. (B3) originate from the excited state internal energy and from the atom-laser coupling term. This latter term can be expressed solely in terms of the atomic field operator $\hat{\chi}_{3D}$ in the coupled internal state $|C\rangle$, as defined in Eq. (42). Along the lines of Ref. [71], we formally integrate $[\partial_t + (-i\delta + \Gamma/2)]\hat{\Psi}_e = \hat{S}$ neglecting a transient of duration $1/\Gamma$ as

$$\hat{\Psi}_e(\mathbf{r},t) = \int_0^{+\infty} d\tau e^{-(-i\delta+\Gamma/2)\tau}\hat{S}(\mathbf{r},t-\tau). \qquad (B4)$$

The Rabi frequencies $\Omega_{c,p}$ and the atomic field $\hat{\chi}_{3D}$ have a negligible variation during $1/\Gamma$ and may be replaced by their values at time t in the integrand. This leads to Eq. (43) of the main text, where the noise term is defined as $\hat{B}_e(\mathbf{r},t) = \int_0^{+\infty} d\tau \, e^{-(-i\delta+\Gamma/2)\tau}\hat{F}_e(\mathbf{r},t-\tau)$.

As explained in Sec. III, we are in a regime where the atoms are mostly in the noncoupled state and the field $\hat{\chi}_{3D}$ in the coupled state is small and a perturbation expansion in powers of $\hat{\chi}_{3D}$ can be performed. The gauge-field formalism discussed in Sec. III for the evolution of the atomic field $\hat{\phi}_{3D}$ in the noncoupled state [defined in Eq. (12)] is already recovered at zeroth order in $\hat{\chi}_{3D}$. From this zeroth-order approximation of $\hat{\phi}_{3D}$, it is then easy to obtain the first-order contribution to

the field $\hat{\chi}_{3D}$ that is required in Sec. V to evaluate the optical polarization of the moving atoms.

From Eq. (12) the equation of motion for $\hat{\phi}_{3D}$ is

$$\partial_t \hat{\phi}_{3D} = \frac{1}{i\hbar}[\hat{\phi}_{3D}, H] + \sum_{\alpha = a, b} \hat{\Psi}_\alpha \partial_t \langle NC | \alpha \rangle. \quad (B5)$$

By the very definition of a noncoupled state, the excited-state internal energy and the atom-laser coupling terms give an exactly vanishing contribution to the commutator. In the other terms of the Hamiltonian, as well as in the last sum in Eq. (B5), we can perform the approximation $\hat{\Psi}_\alpha \simeq \langle \alpha | NC \rangle \hat{\phi}_{3D}$, which is accurate at zeroth order in $\hat{\chi}_{3D}$. After an integration by part and noting that $\langle NC | \partial_t | NC \rangle$ and $\langle NC | \nabla | NC \rangle$ are purely imaginary quantities, we find that up to this order $\hat{\phi}_{3D}$ follows a purely Hamiltonian evolution governed by Eq. (13).

The equation of motion of $\hat{\chi}_{3D}$ has the form

$$\partial_t \hat{\chi}_{3D} = \frac{1}{i\hbar}[\hat{\chi}_{3D}, H] + \sum_{\alpha = a, b} \hat{\Psi}_\alpha \partial_t \langle C | \alpha \rangle. \quad (B6)$$

The commutator with the internal excited-state energy term introduces a $\hat{\Psi}_e$ term that we replace with Eq. (43): In this way, both a noise term and a complex, position-dependent energy term $-(i\delta' + \Gamma'/2)\hat{\chi}_{3D}$ appear in the equation. The real quantities δ' and Γ' are given by Eq. (11) and correspond to light-shift and damping effects, respectively.

Since $\hbar\Gamma'$ is much larger than the kinetic, trapping, interaction, and recoil energies of the atoms, we can neglect these latter terms in the evolution equation of the coupled state and only keep the coupling to $\hat{\phi}_{3D}$. This amounts to keeping in Eq. (B6) only the contributions to the kinetic, trapping, and interaction terms of the Hamiltonian H that contain one single factor $\hat{\chi}_{3D}^\dagger$ and an arbitrary number of $\hat{\phi}_{3D}$ and $\hat{\phi}_{3D}^\dagger$ factors. In this way, we obtain

$$\partial_t \hat{\chi}_{3D} \simeq -\left(i\delta' + \frac{\Gamma'}{2}\right)\hat{\chi}_{3D} + \hat{\phi}_{3D}\langle C|\left[-\partial_t + \frac{i\hbar}{2m}\Delta\right]|NC\rangle$$
$$+ \frac{i\hbar}{m}\nabla\hat{\phi}_{3D} \cdot \langle C|\nabla|NC\rangle + \frac{1}{i\hbar}\mathcal{G}\hat{\phi}_{3D}^\dagger\hat{\phi}_{3D}^2 + \Gamma'^{1/2}\hat{F}_\chi, \quad (B7)$$

where we have introduced a complex position and time-dependent coupling constant

$$\mathcal{G} = \langle C|a\rangle\langle a|NC\rangle[(g_{aa} - g_{ab})\langle NC|a\rangle\langle a|NC\rangle - a \leftrightarrow b] \quad (B8)$$

with the convention $g_{ba} = g_{ab}$. The noise term is defined by $\hat{F}_\chi = -i|\delta + i\Gamma/2|(\Omega_c^*/|\Omega_c|)\hat{B}_e$. Its correlation properties are determined by the commutation relation $[\hat{F}_\chi(\mathbf{r}, t), \hat{F}_\chi^\dagger(\mathbf{r}', t')] \simeq \frac{|\delta + i\Gamma/2|^2}{\Gamma}e^{i(t-t')\delta - \Gamma|t-t'|/2}\delta(\mathbf{r} - \mathbf{r}')$. Since we are working in a low saturation regime in which $\Gamma \gg \Gamma'$, the time-dependent factor in front of $\delta(\mathbf{r} - \mathbf{r}')$ may be replaced with a Dirac of $t - t'$, so $\hat{F}_\chi$ is, in practice, a spatio-temporally δ-correlated noise.

The last step is to expand Eq. (B7) to first order in Ω_p/Ω_c. We also limit ourselves to zeroth order in q/k_p and in $1/(k_p w)$, and we neglect the temporal derivative of the switch-off function $f(t)$. Then, (i) for $g_{aa} \simeq g_{ab}$, the fourth contribution in the right-hand side of Eq. (B7) vanishes [72], and (ii) for

the magic choice Eq. (23), the second contribution in the right-hand side of Eq. (B7) vanishes. With the same adiabatic elimination technique adopted for $\hat{\Psi}_e$ and taking into account the fact that δ' and Γ' vary very slowly on the scale of $1/\Gamma'$, we are finally led to the final equation, Eq. (45), with a noise term defined by $\hat{B}_\chi(\mathbf{r}, t) = \int_0^{+\infty} d\tau e^{-[i\delta' + \Gamma'/2](\mathbf{r}, t)\tau}\hat{F}_\chi(\mathbf{r}, t - \tau)$.

We complete the discussion by giving the back-action of the field $\hat{\chi}_{3D}$ on the field $\hat{\phi}_{3D}$, a back-action that was already considered for a specific single atom geometry in Ref. [28]. The linear coupling of $\hat{\phi}_{3D}$ to $\hat{\chi}_{3D}$ originates from terms in the Hamiltonian that are linear in $\hat{\chi}_{3D}$, leading to

$$(\partial_t \hat{\phi}_{3D})_{\text{back}} = \hat{\chi}_{3D}\langle NC|\left[-\partial_t + \frac{i\hbar}{2m}\Delta\right]|C\rangle$$
$$+ \frac{i\hbar}{m}\nabla\hat{\chi}_{3D} \cdot \langle NC|\nabla|C\rangle + \frac{1}{i\hbar}\left[\mathcal{G}\hat{\chi}_{3D}^\dagger\hat{\phi}_{3D}^2\right.$$
$$\left. + 2\mathcal{G}^*\hat{\phi}_{3D}^\dagger\hat{\phi}_{3D}\hat{\chi}_{3D}\right]. \quad (B9)$$

Expression of the back-action solely in terms of $\hat{\phi}_{3D}$ and noise operators is obtained by replacing $\hat{\chi}_{3D}$ in the resulting equations of motion with its adiabatic approximation derived from Eq. (B7). This leads, in general, to a lengthy formula. For simplicity, we give the result for $g_{aa} = g_{ab}$ to leading order in Ω_p/Ω_c; we also neglect the contribution to $\langle C|\partial_t|NC\rangle$ of the time derivative of the switch-off function $f(t)$, and we use the specific form Ω_p/Ω_c considered in this article, see Eqs. (6) and (7), restricting to zeroth order in q/k_p and $1/(k_p w)$ so

$$(\partial_t \hat{\phi}_{3D})_{\text{back}} \simeq -\frac{i\hbar^2}{m^2}\frac{4(\delta + i\Gamma/2)}{|\Omega_c|^2}\left|\frac{\Omega_p}{\Omega_c}\right|^2$$
$$\times [(\mathbf{k}_p - \mathbf{k}_c) \cdot \nabla]^2 \hat{\phi}_{3D} + \text{noise terms}. \quad (B10)$$

After reduction to the xy plane, the deterministic term gives rise to two corrections to the evolution of $\hat{\phi}_{3D}$: (i) a complex position-dependent energy shift,

$$\hbar(\delta'' - i\Gamma''/2) = -2(\delta + i\Gamma/2)\omega_z \frac{\hbar^2 k_c^2}{m}\frac{|\Omega_p|^2}{|\Omega_c|^4}, \quad (B11)$$

and (ii) a complex correction to the mass along y, $\delta m_y = 8\hbar k_c^2|\Omega_p|^2(\delta + i\Gamma/2)/|\Omega_c|^4$. The quantity $\hbar\delta''$ is the light-shift potential experienced by the noncoupled bidimensional field. The spatial average of the fluorescence rate Γ'' of the noncoupled field coincides with the $\Gamma_{\text{fluo}}^{\text{non-ad}}$ fluorescence rate previously discussed in Eq. (A2), as it should be. For the parameters of Table I, the reactive corrections δ'' and δm_y are small provided that the detuning is not too large, $|\delta/\Gamma| < 5$. For instance, an estimate for the undesired energy deposited by the $\hbar\delta''$ potential can be obtained from the Bogoliubov theory for a homogeneous system, see Eq. (D15), leading to

$$\frac{\Delta E_{\hbar\delta''}}{\Delta E_2} \approx \frac{5 \times 10^{-5}}{f_n}(\delta/\Gamma)^2, \quad (B12)$$

where ΔE_2 is the desired deposited energy giving access to the normal fraction f_n.

APPENDIX C: DERIVATION OF THE EXPRESSION FOR THE DEPOSITED ENERGY

We start from a two-dimensional system at thermal equilibrium with no average current and we apply a gauge field of the form

$$\mathbf{A}(\mathbf{r},t) = f(t)\mathbf{e}_y |c_+ e^{i\mathbf{q}\cdot\mathbf{r}/2} + c_- e^{-i\mathbf{q}\cdot\mathbf{r}/2}|^2 e^{-(\mathbf{r}-\mathbf{r}_0)^2/(2\sigma^2)}, \quad \text{(C1)}$$

where $\mathbf{e}_\alpha$ is the unit vector along direction α. The derivable dimensionless envelope function $f(t)$ is assumed to be zero for $t < 0$ and to rapidly tend to zero for $t \to +\infty$. The time-independent coefficients $c_\pm$ have the dimension of the square root of a momentum.

We are interested in evaluating the energy change of the system from $t = 0^-$ to $t = +\infty$ at the lowest order in $c_\pm$. We work in the Schrödinger picture and we first use the exact relations:

$$\Delta E \equiv \int_{-\infty}^{+\infty} dt \, \frac{d\langle H(t)\rangle}{dt} \quad \text{(C2)}$$

$$= \int_{-\infty}^{+\infty} dt \int d^2 r \, \mathbf{A}(\mathbf{r},t) \cdot \frac{d}{dt} \langle \mathbf{j}(\mathbf{r})\rangle(t), \quad \text{(C3)}$$

where the second equality comes from a time-dependent Hellmann-Feynman theorem and a temporal integration by parts. Calculating $\langle \mathbf{j}(\mathbf{r})\rangle(t)$ by linear response theory gives

$$\Delta E \simeq \int_{\mathbb{R}} \frac{d\omega}{2\pi} \int d^2 r \int d^2 r' \, \omega$$

$$\times \text{Im}\left[\sum_{\alpha,\beta} \chi_{\alpha\beta}^{\text{ex}}(\mathbf{r},\mathbf{r}';\omega) A_\alpha(\mathbf{r},\omega)^* A_\beta(\mathbf{r}',\omega) \right], \quad \text{(C4)}$$

where χ^{ex} is the exact current susceptibility in real space, taking into account the spatial inhomogeneity of the trapped cloud. Note that, contrarily to Eq. (C2), Eqs. (C3) and (C4) still hold when $f(t) = 0$ for $t < 0$ and has a discontinuous jump in $t = 0$.

We now use the particular form (C1) for $\mathbf{A}$ and consider the relevant limiting case $q\sigma \gg 1$, $q \min(\xi,\lambda) \ll 1$, where ξ is the healing length of the gas and λ is the thermal de Broglie wavelength. We also assume that σ is much smaller than the radius of the trapped cloud, so the density variation within a region of radius σ around $\mathbf{r}_0$ may be neglected.

Within a local-density approximation, we then replace χ^{ex} with the susceptibility χ of a spatially homogeneous system with a density equal to the one of the trapped gas at position $\mathbf{r}_0$ and with the same temperature, $\chi^{\text{ex}}(\mathbf{r},\mathbf{r}';\omega) \simeq \chi(\mathbf{r}-\mathbf{r}';\omega)$.

This local-density approximation leads to

$$\Delta E \simeq \int_{\mathbb{R}} \frac{d\omega}{2\pi} \omega \, |f(\omega)|^2 \int d^2 R \int d^2 u \, [|c_+|^2 + |c_-|^2$$

$$+ c_+^* c_- e^{-i\mathbf{q}\cdot(\mathbf{R}+\mathbf{u}/2)} + c_+ c_-^* e^{i\mathbf{q}\cdot(\mathbf{R}+\mathbf{u}/2)}]$$

$$\times [|c_+|^2 + |c_-|^2 + c_+^* c_- e^{-i\mathbf{q}\cdot(\mathbf{R}-\mathbf{u}/2)} + c_+ c_-^* e^{i\mathbf{q}\cdot(\mathbf{R}-\mathbf{u}/2)}]$$

$$\times \text{Im}[\chi_{yy}(\mathbf{u};\omega)] \, e^{-|\mathbf{R}-\mathbf{r}_0|^2/\sigma^2} e^{-u^2/(4\sigma^2)}, \quad \text{(C5)}$$

where we have performed the change of variables $\mathbf{r} = \mathbf{R} + \mathbf{u}/2, \mathbf{r}' = \mathbf{R} - \mathbf{u}/2$. As we work in the $q\sigma \gg 1$ regime, we have, for example,

$$\int d^2 R \, e^{-2i\mathbf{q}\cdot\mathbf{R}} e^{-|\mathbf{R}-\mathbf{r}_0|^2/\sigma^2} = e^{-2i\mathbf{q}\cdot\mathbf{R}_0} \pi \sigma^2 e^{-q^2\sigma^2} \ll \pi\sigma^2 \quad \text{(C6)}$$

so all the oscillating terms in $\mathbf{R}$ may be neglected. Introducing the Fourier transform of $\chi_{yy}(\mathbf{k};\omega)$, which is an even function of $\mathbf{k}$ due to parity or rotational invariance, we obtain

$$\Delta E = \Delta E_1 + \Delta E_2, \quad \text{(C7)}$$

$$\Delta E_1 \simeq \int_{-\infty}^{+\infty} \frac{d\omega}{2\pi} \omega |f(\omega)|^2 (2\pi\sigma^2)^2 \int \frac{d^2 k}{(2\pi)^2}$$

$$\times \text{Im} \, \chi_{yy}(\mathbf{k};\omega)(|c_+|^2 + |c_-|^2)^2 e^{-k^2\sigma^2}, \quad \text{(C8)}$$

$$\Delta E_2 \simeq \int_{-\infty}^{+\infty} \frac{d\omega}{2\pi} \omega |f(\omega)|^2 (2\pi\sigma^2)^2 \int \frac{d^2 k}{(2\pi)^2}$$

$$\times \text{Im} \, \chi_{yy}(\mathbf{q}+\mathbf{k};\omega) 2|c_+|^2 |c_-|^2 e^{-k^2\sigma^2}. \quad \text{(C9)}$$

The second contribution ΔE_2 comes from the spatially modulated gauge field at $\mathbf{q}$, while the first contribution ΔE_1 is due to the nonmodulated term which follows the broad Gaussian envelope. Expression (24) in the main text is obtained from (C9) by noting that the integration over $\mathbf{k}$ is effectively limited by the Gaussian factor to a small region of radius $1/\sigma$ in which one is allowed to neglect the $\mathbf{k}$ dependence of the susceptibility.

Naively, one could guess that a necessary condition for the accuracy of our local-density approximation is that the switch-off time of the gauge field γ^{-1} is short as compared to the characteristic time $2R/v$ for the induced mechanical perturbation to cross the whole cloud, to be reflected by its boundaries, and to turn back to the excitation zone where it can interfere with the excitation process, v being the fastest between the sound and thermal speeds in the cloud of radius R.

This condition is actually sufficient, but not necessary, within linear response theory. We now show for $f(t) = \Theta(t)e^{-\gamma t}$, as in Eq. (27), that the $\gamma \to 0$ limit for the deposited energy scheme exists and coincides with the perturbation induced by the gauge field in the thermodynamic equilibrium state. As one can show by inserting the explicit form of the temporal Fourier transform of the gauge field into (C4) and performing the integral over ω, the deposited energy can be written in the form

$$\Delta E \simeq \frac{1}{2} \int d^2 r \, d^2 r' \sum_{\alpha,\beta} A_\alpha(\mathbf{r},t=0^+) \, A_\beta(\mathbf{r}',t=0^+)$$

$$\times \text{Re}[\chi_{\alpha\beta}^{\text{ex}}(\mathbf{r},\mathbf{r}';\omega = i\gamma)], \quad \text{(C10)}$$

where we have introduced the Kubo formula for the exact current-current susceptibility

$$\chi_{\alpha\beta}^{\text{ex}}(\mathbf{r},\mathbf{r}';\omega) = \sum_{\lambda,\lambda'} (\pi_\lambda - \pi_{\lambda'}) \frac{\langle\lambda|j_\alpha(\mathbf{r})|\lambda'\rangle\langle\lambda'|j_\beta(\mathbf{r}')|\lambda\rangle}{E_{\lambda'} - E_\lambda - \hbar\omega - i0^+} \quad \text{(C11)}$$

in terms of the thermal equilibrium population π_λ of quantum state λ. This quantity can be simply related to the susceptibility at thermodynamic equilibrium,

$$\chi_{\alpha\beta}^{\text{th}}(\mathbf{r},\mathbf{r}') = \lim_{\gamma\to 0} \text{Re}[\chi_{\alpha\beta}^{\text{ex}}(\mathbf{r},\mathbf{r}';\omega = i\gamma)]$$

$$+ \frac{1}{k_B T} \sum_{\lambda,\lambda';E_\lambda=E_{\lambda'}} \pi_\lambda \langle\lambda|j_\alpha(\mathbf{r})|\lambda'\rangle\langle\lambda'|j_\beta(\mathbf{r}')|\lambda\rangle. \quad \text{(C12)}$$

We recall that the thermodynamic susceptibility relates the mean current in a thermal equilibrium state at temperature

T to the applied (weak) static gauge field via $\langle \mathbf{j} \rangle = \chi^{\text{th}} * \mathbf{A}$, where $*$ is the spatial convolution product. In the present case of an interacting gas, one can safely expect that the second line in Eq. (C12) gives a negligible contribution as there is no systematic degeneracy and the current operator $\mathbf{j}$ has no diagonal matrix elements since the eigenstate wave functions may be taken as real. Within linear response theory, we thus obtain

$$\Delta E \underset{\gamma \to 0}{\longrightarrow} \frac{1}{2} \int d^2 r \, d^2 r' \sum_{\alpha,\beta} \chi^{\text{th}}_{\alpha\beta}(\mathbf{r},\mathbf{r}') A_\alpha(\mathbf{r},0^+) A_\beta(\mathbf{r}',0^+).$$

(C13)

Since local-density approximation in the thermodynamic equilibrium state is a standard procedure, we expect that it can be applied to evaluate the right-hand side of Eq. (C13) [73]. As a consequence, within linear response theory, our deposited energy method [that measures the left-hand side of Eq. (C13)] should be accurately described by the local-density approximation down to the $\gamma \to 0$ limit.

APPENDIX D: SOME RESULTS OF LINEAR RESPONSE THEORY AND THE BOGOLIUBOV EXPRESSION OF THE DEPOSITED ENERGY

A system of time-independent Hamiltonian H_0 experiences, at times $t > 0$, a time-dependent weak perturbation of Hamiltonian $-\epsilon f(t) \mathcal{V}$, where $\epsilon \to 0$, the dimensionless time-dependent factor $f(t)$ is zero for $t < 0$ and tends rapidly to zero for $t \to +\infty$, and the operator $\mathcal{V}$ is time independent. At time $t = +\infty$, the system is free again, with a mean energy modified by the perturbation. The question is to calculate the mean energy change to second order in ϵ.

Suppose, first, that, at $t = 0^-$, the system is prepared in the eigenstate $|\lambda\rangle$ of H_0 of eigenenergy E_λ. The energy change δE between time 0 and time $+\infty$ is

$$\delta E = \lim_{t \to +\infty} \langle \psi(t) | (H_0 - E_\lambda) | \psi(t) \rangle, \qquad (D1)$$

where $|\psi(t)\rangle$ is the system state vector at time t. The usual time-dependent perturbation theory gives an expansion in powers of ϵ:

$$|\psi(t)\rangle = |\psi_0(t)\rangle + \epsilon|\psi_1(t)\rangle + \epsilon^2|\psi_2(t)\rangle + \dots, \quad (D2)$$

where $|\psi_0(t)\rangle = \exp(-i E_\lambda t/\hbar)|\lambda\rangle$,

$$|\psi_1(t)\rangle = -\int_0^t \frac{d\tau}{i\hbar} e^{-i H_0(t-\tau)/\hbar} f(\tau) \mathcal{V} e^{-i E_\lambda \tau/\hbar} |\lambda\rangle, \quad (D3)$$

and the expression of higher-order contributions is not needed. Using $(H_0 - E_\lambda)|\psi_0(t)\rangle = 0$ and $\langle \psi_0(t)|(H_0 - E_\lambda) = 0$, we find to second order in ϵ,

$$\delta E \simeq \lim_{t \to +\infty} \epsilon^2 \langle \psi_1(t)|(H_0 - E_\lambda)|\psi_1(t)\rangle. \qquad (D4)$$

In this article, $f(t) = \Theta(t) \exp(-\gamma t)$, with $\gamma > 0$, and $\Theta(t)$ is the Heaviside step function, see Eq. (27). Also, the system is prepared initially in a statistical mixture of eigenstates of H_0 with a probability distribution π_λ. After explicit integration of

(D3) over τ and then average over $|\lambda\rangle$, the expression for the signal to be detected experimentally is

$$\begin{aligned} \text{Signal}\,(\mathcal{V}) &\equiv \lim_{\epsilon \to 0} \frac{\langle \delta E \rangle}{\epsilon^2} \\ &= \frac{1}{2} \operatorname{Re} \sum_{\lambda,\lambda'} \frac{(\pi_\lambda - \pi_{\lambda'})}{E_{\lambda'} - E_\lambda - i\hbar\gamma} |\langle \lambda' | \mathcal{V} | \lambda \rangle|^2. \quad (D5) \end{aligned}$$

The sum may be restricted to $E_\lambda \neq E_{\lambda'}$ since the contributions with $E_\lambda = E_{\lambda'}$ are zero. This also shows that the signal has a finite limit for $\gamma \to 0^+$. Note that in a thermal equilibrium state $\pi_\lambda = Z^{-1} \exp(-E_\lambda/k_B T)$, the signal is necessarily positive.

The calculation of the noise on the experimental signal can be performed along the same lines. One defines $\delta E^2 \equiv \lim_{t \to +\infty} \langle \psi(t)|(H_0 - E_\lambda)^2|\psi(t)\rangle$ with the initial state vector $|\psi(0)\rangle = |\lambda\rangle$, and one finds after averaging over the initial state:

$$\begin{aligned} [\text{Noise}\,(\mathcal{V})]^2 &\equiv \lim_{\epsilon \to 0} \frac{\langle \delta E^2 \rangle}{\epsilon^2} \underset{\gamma \to 0}{=} \sum_{\lambda,\lambda',E_\lambda \neq E'_\lambda} \pi_\lambda |\langle \lambda | \mathcal{V} | \lambda' \rangle|^2 \\ &\simeq \sum_\lambda \pi_\lambda [\langle \lambda | \mathcal{V}^2 | \lambda \rangle - \langle \lambda | \mathcal{V} | \lambda \rangle^2], \quad (D6) \end{aligned}$$

where the approximate equality is based on the assumption that there are no systematic degeneracies in the many-body spectrum. The ϵ^2 scaling of the variance in Eq. (D6) shows that the typical value of the energy change at the end of the excitation sequence is of order ϵ. This scaling is to be contrasted with the ϵ^2 one of the expectation value that is suggested by Eq. (D5).

We now apply the general formula Eq. (D5) to the Bogoliubov analysis of Sec. IV B. In this case, $\epsilon = \epsilon_{\text{gauge}}/2$ and $\mathcal{V} = \mathcal{V}_q + \mathcal{V}_{-q}$ with

$$\mathcal{V}_q = \int_{[0,L]^2} d^2 r \, e^{iqx} j_y(\mathbf{r}) = \sum_{\mathbf{k}} \frac{\hbar k_y}{m} a^\dagger_{\mathbf{k}+\mathbf{q}} a_{\mathbf{k}}, \qquad (D7)$$

where $a_{\mathbf{k}}$ is the annihilation operator of a particle of the gas of wave vector $\mathbf{k}$, and we have set $\mathbf{q} = q\,\mathbf{e}_x$. In a translationally invariant system, the eigenstates $|\lambda\rangle$ can be taken of well-defined total momentum; as the action of $\mathcal{V}_{\pm q}$ changes this total momentum by $\pm\hbar\mathbf{q}$, the two operators $\mathcal{V}_q$ and $\mathcal{V}_{-q}$ cannot interfere in the signal and thus $\text{Signal}(\mathcal{V}) = 2\,\text{Signal}(\mathcal{V}_q)$. In terms of the annihilation operators $b_{\mathbf{k}}$ of Bogoliubov quasiparticles, we can split

$$\mathcal{V}_q = \mathcal{V}_q^{(0)} + \mathcal{V}_q^{(2)} + \mathcal{V}_q^{(-2)} \qquad (D8)$$

in terms of

$$\mathcal{V}_q^{(0)} = \sum_{\mathbf{k} \neq \mathbf{0}, -\mathbf{q}} \frac{\hbar k_y}{m} (U_{\mathbf{k}} U_{\mathbf{k}+\mathbf{q}} - V_{\mathbf{k}} V_{\mathbf{k}+\mathbf{q}}) \, b^\dagger_{\mathbf{k}+\mathbf{q}} b_{\mathbf{k}}, \quad (D9)$$

$$\mathcal{V}_q^{(2)} = \sideset{}{'}\sum_{\mathbf{k} \neq \mathbf{0}, -\mathbf{q}} \frac{\hbar k_y}{m} (V_{\mathbf{k}} U_{\mathbf{k}+\mathbf{q}} - U_{\mathbf{k}} V_{\mathbf{k}+\mathbf{q}}) \, b^\dagger_{\mathbf{k}+\mathbf{q}} b^\dagger_{-\mathbf{k}}, \quad (D10)$$

$$\mathcal{V}_q^{(-2)} = \sideset{}{'}\sum_{\mathbf{k} \neq \mathbf{0}, -\mathbf{q}} \frac{\hbar k_y}{m} (U_{\mathbf{k}} V_{\mathbf{k}+\mathbf{q}} - V_{\mathbf{k}} U_{\mathbf{k}+\mathbf{q}}) \, b_{\mathbf{k}} b_{-(\mathbf{k}+\mathbf{q})}. \quad (D11)$$

The primed sum $\sum'$ indicates restriction of the sum over wave vectors such that $k_y > 0$. In Bogoliubov theory, the eigenstates $|\lambda\rangle$ may be taken in the form of Fock states of quasiparticles.

Since $\mathcal{V}_q^{(n)}$ changes the total number of quasiparticles by the amount n, the terms in the right-hand side of Eq. (D8) cannot interfere in the signal and

$$\text{Signal}(\mathcal{V}_q) = \text{Signal}(\mathcal{V}_q^{(0)}) + \text{Signal}(\mathcal{V}_q^{(2)}) + \text{Signal}(\mathcal{V}_q^{(-2)}).$$
(D12)

Thanks to the clever writing of $\mathcal{V}_q^{(n)}$ with the constraint $k_y > 0$ [74], there are no interferences in Eqs. (D9)–(D11) between the different terms of the sums over $\mathbf{k}$. As a result, the whole signal is the sum over the contribution of the different $\mathbf{k}$'s. The last trick is to express the ratios $\pi_{\lambda'}/\pi_\lambda$ in terms of the mean occupation numbers $n_\mathbf{k}$ of the Bogoliubov modes of energy $\epsilon_\mathbf{k}$ and to make use of the identity

$$e^{\beta\epsilon_\mathbf{k}} = \frac{n_\mathbf{k}+1}{n_\mathbf{k}}$$
(D13)

satisfied by the Bose law. A little bit of rewriting, taking advantage of the relation $\text{Signal}(\mathcal{V}) = (N/m)f_n^{\text{eff}}$ and of the remarks in Ref. [74], finally leads to Eq. (31).

An alternative procedure is to calculate the current-current susceptibility (C11) for a spatially homogeneous system within the Bogoliubov theory, which for $\mathbf{q} \perp \mathbf{e}_y$ gives in dimension d the following:

$$\chi_{yy}(\mathbf{q};\omega)$$
$$= \frac{1}{L^d} \sum_{\mathbf{k}\neq 0,-\mathbf{q}} \frac{\hbar^2 k_y^2}{m^2}$$
$$\times \left[\frac{n_\mathbf{k} - n_{\mathbf{k}+\mathbf{q}}}{\epsilon_{\mathbf{k}+\mathbf{q}} - \epsilon_\mathbf{k} - \hbar\omega - i0^+} (U_{\mathbf{k}+\mathbf{q}}^2 U_\mathbf{k}^2 - U_{\mathbf{k}+\mathbf{q}} V_{\mathbf{k}+\mathbf{q}} U_\mathbf{k} V_\mathbf{k}) \right.$$
$$- \frac{1 + n_\mathbf{k} + n_{\mathbf{k}+\mathbf{q}}}{-\epsilon_{\mathbf{k}+\mathbf{q}} - \epsilon_\mathbf{k} - \hbar\omega - i0^+} (V_{\mathbf{k}+\mathbf{q}}^2 U_\mathbf{k}^2 - U_{\mathbf{k}+\mathbf{q}} V_{\mathbf{k}+\mathbf{q}} U_\mathbf{k} V_\mathbf{k})$$
$$+ \frac{1 + n_\mathbf{k} + n_{\mathbf{k}+\mathbf{q}}}{\epsilon_{\mathbf{k}+\mathbf{q}} + \epsilon_\mathbf{k} - \hbar\omega - i0^+} (U_{\mathbf{k}+\mathbf{q}}^2 V_\mathbf{k}^2 - U_{\mathbf{k}+\mathbf{q}} V_{\mathbf{k}+\mathbf{q}} U_\mathbf{k} V_\mathbf{k})$$
$$+ \left. \frac{n_{\mathbf{k}+\mathbf{q}} - n_\mathbf{k}}{\epsilon_\mathbf{k} - \epsilon_{\mathbf{k}+\mathbf{q}} - \hbar\omega - i0^+} (V_{\mathbf{k}+\mathbf{q}}^2 V_\mathbf{k}^2 - U_{\mathbf{k}+\mathbf{q}} V_{\mathbf{k}+\mathbf{q}} U_\mathbf{k} V_\mathbf{k}) \right].$$
(D14)

From Eq. (C4) one then recovers expression Eq. (31) for the effective normal fraction f_n^{eff}.

Another application of Eq. (D5) is to calculate the energy deposited by the external potential $\mathcal{U}(\mathbf{r},t) = (\mathcal{U}_0 e^{i\mathbf{Q}\cdot\mathbf{r}} + \text{c.c.})\Theta(t)e^{-\eta t}$ in the spatially homogeneous case for $\eta > 0$. This is useful for Appendix A and Appendix B to estimate the effect of undesired light shifts. In the second quantized form, and to leading order in Bogoliubov theory, one then has $\epsilon\mathcal{V} = N^{1/2}(U_Q + V_Q)[\mathcal{U}_0(b_\mathbf{Q}^\dagger + b_{-\mathbf{Q}}) + \text{H.c.}]$. These terms do not interfere in Eq. (D5). For nonzero temperature, using (D13), we then obtain a temperature-independent result,

$$\Delta E_\mathcal{U} \simeq 2N|\mathcal{U}_0|^2 (U_Q + V_Q)^2 \text{Re}\left[\frac{1}{\epsilon_Q - i\hbar\eta}\right]. \quad \text{(D15)}$$

Remarkably, this also allows us to calculate the energy change ΔE_g due to the switch-on-and-off of a spatially modulated coupling constant, $\delta g(\mathbf{r},t) = (\delta g_0 e^{i\mathbf{q}\cdot\mathbf{r}} + \text{c.c.})\Theta(t)e^{-\gamma t}$. For a spatially homogeneous system, to leading order of Bogoliubov theory, the relevant operator is $\epsilon\mathcal{V} = N^{1/2}(U_q + V_q)[\rho\delta g_0(b_\mathbf{q}^\dagger + b_{-\mathbf{q}}) + \text{H.c.}]$, so one can formally apply

Eq. (D15) with $\mathcal{U}_0 = \rho\delta g_0$. This can be applied to the variation of the coupling constant due to $g_{aa} \neq g_{ab}$ in Eq. (18). In this case, $\delta g_0 = 2g[(g_{ab} - g_{aa})/g_{aa}](\Omega_p^+ \Omega_p^{-*})(0^+)/|\Omega_c|^2$ so, for $q\xi = 1$ and $\gamma \to 0$,

$$\frac{\Delta E_g}{\Delta E_2} \simeq \frac{16}{5f_n} \frac{m\rho g}{(\hbar k_c)^2} \left(\frac{g_{ab} - g_{aa}}{g_{aa}}\right)^2. \quad \text{(D16)}$$

For the values of Table I and $|g_{ab} - g_{aa}| \lesssim 0.1|g_{aa}|$ as expected for ^{87}Rb, this gives $\Delta E_g/\Delta E_2 \approx 7 \times 10^{-4}/f_n$, which is negligible.

APPENDIX E: THE NOISE ON THE DEPOSITED ENERGY

In Sec. IV C, while presenting the numerical results on the deposited energy measurement, we mentioned that the statistical noise on the deposited energy was larger for smaller values of the gauge-field amplitude ϵ_{gauge}.

To understand this feature, it can be useful to rewrite the deposited energy for a single realization of the classical field simulation in the form

$$\delta E = -\int d^2r\, \mathbf{j}(\mathbf{r},0) \cdot \mathbf{A}(\mathbf{r},0^+) - \int_{0^+}^{+\infty} dt$$
$$\times \int d^2r\, \mathbf{j}(\mathbf{r},t)\, \partial_t \mathbf{A}(\mathbf{r},t). \quad \text{(E1)}$$

The first term comes from the abrupt switch-on of the gauge field. For each realization, it is of order ϵ_{gauge} but averages to zero in the limit of an infinite number of realizations of the experiment as $\langle\mathbf{j}(\mathbf{r},0)\rangle = 0$. In any actual calculation, an average over a finite number n_{real} of realizations is taken, which gives a nonzero random value for δE scaling as $\epsilon_{\text{gauge}}/\sqrt{n_{\text{real}}}$.

The relevant signal $\langle\delta E\rangle$ is given by the second term in Eq. (E1), obtained from the classical Hamiltonian identity $dH/dt = \partial_t H$. For small values of the gauge-field switch-off rate γ, this term is of order $O(\epsilon_{\text{gauge}}^2)$ as in this limit $\mathbf{j}$ adiabatically follows the thermal equilibrium value for the instantaneous value of the gauge field. As a result, the number of realizations that are needed to extract the signal out of the statistical noise due to the first term grows as $|\epsilon_{\text{gauge}}|^{-2}$, which perfectly explains the numerical observation.

Furthermore, it has been demonstrated by a number of recent cold-atom experiments that noise is not always just an hindrance but can be also a source of useful physical information [75,76]. As a simple example, we consider here the amplitude of the noise on the energy that is deposited in the system at each realization of the experiment. This quantity is quantified by the average $\langle\delta E^2\rangle$ of the square of the deposited energy in the $\gamma \to 0$ limit. Looking at Eq. (E1), it is immediate to see that in the small ϵ_{gauge} limit the dominant contribution comes from the square of the first term, which suggests that the noise on the deposited energy is related to the variance of the instantaneous fluctuations of the current operator. From the fluctuation-dissipation theorem, this quantity can then be related to the normal fraction of the gas.

This idea can be put on solid ground by developing a full quantum calculation. The linear response theory calculation

performed along the lines of Appendix D leads to the expression in Heisenberg picture as follows:

$$\lim_{\gamma \to 0} \langle [H_0(+\infty) - H_0(0)]^2 \rangle$$
$$\simeq \left\langle \left[\int d^2r \, \mathbf{j(r)} \cdot \mathbf{A(r,}0^+) \right]^2 \right\rangle, \qquad (E2)$$

where H_0 is the unperturbed Hamiltonian, that is, the Hamiltonian without coupling to the gauge field. This relation connects the variance of the quantum equivalent of the deposited energy to the instantaneous fluctuations of the current operator and confirms our expectation based on the classical field model. Moreover, combined with the fluctuation-dissipation theorem, it can be the starting point for another proposal to measure f_n.

For a generic Hermitian operator V with vanishing diagonal matrix elements in the eigenbasis of H_0, the fluctuation-dissipation theorem of linear response theory relates the imaginary part of the susceptibility χ to the Fourier transform of the correlation function $S_{VV}(t) = \langle V(t) V(0) \rangle$,

$$\text{Im}[\chi_{VV}(\omega)] = \frac{1}{2\hbar} S_{VV}(\omega)[1 - e^{-\hbar\omega/k_BT}]. \qquad (E3)$$

The Fourier transform $S_{VV}(\omega)$ of the correlation function in the thermodynamic equilibrium state is defined as usual as

$$S_{VV}(\omega) = \int_{-\infty}^{\infty} dt \, e^{i\omega t} \langle V(t) V(0) \rangle. \qquad (E4)$$

Under the assumption that most of the spectral weight of the V operator lies in the low-energy region $\hbar\omega \ll k_BT$, we can approximate $1 - e^{-\hbar\omega/k_BT} \simeq \hbar\omega/k_BT$. This is a quite standard approximation of many-body theory and is generally accurate

in the small q limit [77]. After a few manipulations, it leads to the general expression

$$S_{VV}(t = 0) = \int \frac{d\omega}{2\pi} S_{VV}(\omega) \simeq \int \frac{d\omega}{2\pi} \frac{2k_BT}{\omega} \text{Im}[\chi_{VV}(\omega)]$$
$$= k_BT \, \text{Re}[\chi_{VV}(\omega = 0)], \qquad (E5)$$

where the equivalent of Eq. (26) was used to obtain the last identity. An application of the fluctuation-dissipation relation (E5) to the susceptibility and the fluctuations of the mass current in liquid He can be found in Ref. [15].

The link between the variance of the deposited energy and the normal fraction is immediately obtained by applying (E5) to the specific operator

$$V = - \int d^2r \, \mathbf{j(r)} \cdot \mathbf{A(r,}0^+) \qquad (E6)$$

and isolating the contribution of the spatially modulated gauge field proportional to $\Omega_p^+ \Omega_p^-$. In this way, using Eq. (C10), one is led to the final expression

$$\frac{\pi w^2}{4} \frac{\rho}{m} \left(\frac{\epsilon_{\text{gauge}}}{2} \right)^2 f_n \simeq \frac{1}{2k_BT} \lim_{\gamma \to 0} \langle [H_0(+\infty) - H_0(0)]^2 \rangle,$$
$$(E7)$$

which demonstrates an alternative way of extracting the value of the normal fraction f_n from a measurement of the statistical variance of the deposited energy in a series of experiments.

It is, however, crucial to note that a measurement of f_n based on the relation (E7) requires taking expectation values of the Hamiltonian operator at different times. This may be experimentally challenging as it requires either a nondestructive measurement of the initial energy of the system at $t = 0$ before switching on the gauge field or a very precise *a priori* knowledge of its value in a sort of microcanonical ensemble [78].

[1] V. L. Berezinskii, Zh. Eksp. Teor. Fiz. **61**, 1144 (1971) [Sov. Phys. JETP **34**, 610 (1972)]; J. M. Kosterlitz and D. J. Thouless, J. Phys. C **5**, L124 (1972); **6**, 1181 (1973); J. M. Kosterlitz, *ibid.* **7**, 1047 (1974).

[2] P. Minnhagen, Rev. Mod. Phys. **59**, 1001 (1987).

[3] M. Chester and L. C. Yang, Phys. Rev. Lett. **31**, 1377 (1973); D. J. Bishop and J. D. Reppy, *ibid.* **40**, 1727 (1978).

[4] Z. Hadzibabic, P. Krüger, M. Cheneau, B. Battelier, and J. Dalibard, Nature **441**, 1118 (2006).

[5] V. Schweikhard, S. Tung, and E. A. Cornell, Phys. Rev. Lett. **99**, 030401 (2007).

[6] P. Cladé, C. Ryu, A. Ramanathan, K. Helmerson, and W. D. Phillips, Phys. Rev. Lett. **102**, 170401 (2009).

[7] I. Carusotto, Physics **3**, 5 (2010).

[8] N. R. Cooper and Z. Hadzibabic, Phys. Rev. Lett. **104**, 030401 (2010); S. T. John, Z. Hadzibabic, and N. R. Cooper, Phys. Rev. A **83**, 023610 (2011).

[9] T.-L. Ho and Q. Zhou, Nat. Phys. **6**, 131 (2009).

[10] S. P. Rath, T. Yefsah, K. J. Günter, M. Cheneau, R. Desbuquois, M. Holzmann, W. Krauth, and J. Dalibard, Phys. Rev. A **82**, 013609 (2010).

[11] Experimentally, thermal equilibrium in the rotating frame is not always granted. Most likely, it was not achieved in the

experiments of Ref. [12] where the vortex lattices did not nucleate at the expected Landau critical rotation frequency but, rather, at a higher rotation frequency when a dynamical instability of the condensate was triggered [13]. This picture was confirmed by numerical simulations [38].

[12] K. W. Madison, F. Chevy, W. Wohlleben, and J. Dalibard, Phys. Rev. Lett. **84**, 806 (2000); K. Madison, F. Chevy, V. Bretin, and J. Dalibard, *ibid.* **86**, 4443 (2001).

[13] S. Sinha and Y. Castin, Phys. Rev. Lett. **87**, 190402 (2001).

[14] D. Pines and P. Nozières, *The Theory of Quantum Liquids* (Benjamin, New York, 1966), Vol. I; P. Nozières and D. Pines, *The Theory of Quantum Liquids* (Addison-Wesley, Reading, MA, 1990), Vol. II.

[15] F. Dalfovo and S. Stringari, Phys. Rev. B **46**, 13991 (1992).

[16] R. Dum and M. Olshanii, Phys. Rev. Lett. **76**, 1788 (1996).

[17] F. Gerbier and J. Dalibard, New J. Phys. **12**, 033007 (2010).

[18] Y.-J. Lin, R. L. Compton, A. R. Perry, W. D. Phillips, J. V. Porto, and I. B. Spielman, Phys. Rev. Lett. **102**, 130401 (2009).

[19] Y.-J. Lin, R. L. Compton, K. Jiménez-García, J. V. Porto, and I. B. Spielman, Nature **462**, 628 (2009).

[20] S. Nascimbène, N. Navon, K. Jiang, F. Chevy, and C. Salomon, Nature **463**, 1057 (2010); N. Navon, S. Nascimbène, F. Chevy, and C. Salomon, Science **328**, 729 (2010).

[21] S. P. Rath, T. Yefsah, K. J. Günter, M. Cheneau, R. Desbuquois, M. Holzmann, W. Krauth, and J. Dalibard, Phys. Rev. A **82**, 013609 (2010); T. Yefsah, R. Desbuquois, L. Chomaz, K. J. Günter, and J. Dalibard, e-print arXiv:1106.0188.

[22] Mark J. H. Ku, Ariel T. Sommer, Lawrence W. Cheuk, and Martin W. Zwierlein, e-print arXiv:1110.3309; K. Van Houcke, F. Werner, E. Kozik, N. Prokof'ev, B. Svistunov, M. Ku, A. Sommer, L. W. Cheuk, A. Schirotzek, and M. Zwierlein, e-print arXiv:1110.3747 (2011).

[23] E. D. Kuhnle, H. Hu, X.-J. Liu, P. Dyke, M. Mark, P. D. Drummond, P. Hannaford, and C. J. Vale, Phys. Rev. Lett. **105**, 070402 (2010).

[24] E. D. Kuhnle, S. Hoinka, P. Dyke, H. Hu, P. Hannaford, and C. J. Vale, e-print arXiv:1012.2626.

[25] Note that the current operator $\mathbf{j}(\mathbf{r})$ has to be distinguished from the physical current $\mathbf{j}_{\text{phys}} = \mathbf{j} - \mathbf{A}\hat{\phi}^\dagger\hat{\phi}/m$, corresponding to mass transport.

[26] S. Grebenev, M. Hartmann, A. Lindinger, N. Pörtner, B. Sartakov, J. P. Toennies, and A. F. Vilesov, Physica B **280**, 65 (2000).

[27] The probe beams Gaussian profiles are at angles $O(q/k_p)$ with respect to the $z = 0$ plane. However, the resulting z dependence of $\Omega_p^\pm$ can be safely neglected as it occurs on a length-scale $O(wk_p/q)$ much larger than the spatial extension a_{ho}^z of the atomic cloud along z.

[28] A. Aspect, E. Arimondo, R. Kaiser, N. Vansteenkiste, and C. Cohen-Tannoudji, Phys. Rev. Lett. **61**, 826 (1988).

[29] Note that the $-\int \mathbf{j}_{3D} \cdot \mathbf{A}_{3D}$ gauge Hamiltonian is equivalent to the first-quantized form $-\sum_{j=1}^N [\mathbf{p}_j \cdot \mathbf{A}_{3D}(\mathbf{r}_j) + \mathbf{A}_{3D}(\mathbf{r}_j) \cdot \mathbf{p}_j]/2m$, where N is the particle number. Differing from Ref. [16], our scalar potential W_{3D} includes the A_{3D}^2 term.

[30] C. W. Gardiner, and P. Zoller, *Quantum Noise* (Springer, Berlin, 2004).

[31] For the choice (23), to zeroth order in q/k_p and $1/(k_p w)$, W actually vanishes to all orders in Ω_p/Ω_c. To order $(q/k_p)^2$, it does not vanish and scales as $-\hbar^2 q^2 |\Omega_p/\Omega_c|^2/(4m)$, which gives for the parameters of Table I a negligible contribution $\Delta E_W/\Delta E_2 \approx 10^{-3}/f_n$ to the deposited energy scheme.

[32] The spatiotemporal dependence of $g_{3D}(\mathbf{r},t) = g_{aa} + \Delta g(\mathbf{r},t) \simeq g_{aa} + 2(g_{ab} - g_{aa})|\Omega_p(\mathbf{r},t)/\Omega_c|^2$ is responsible for spurious excitation of the gas via two different effects that can be captured by a Bogoliubov treatment. (i) An effective external potential appears of the form $\Delta V_g(\mathbf{r},t) = \rho_{3D}\Delta g(\mathbf{r},t)$: its spatially modulated part at $\pm\mathbf{q}$ is able to excite phonons. (ii) The spatial modulation of the interaction constant that is switched on and off is able to excite pairs of phonons by a parametric down-conversion effect [33]. For suitable atomic species such that $g_{aa} \simeq g_{ab}$ (in particular Rb atoms), the spurious deposited energy turns out to be smaller than the quantity ΔE_2 to be measured (see Appendix D for the analysis of the second contribution).

[33] T. Stöferle, H. Moritz, C. Schori, M. Köhl, and T. Esslinger, Phys. Rev. Lett. **92**, 130403 (2004); M. Krämer, C. Tozzo, and F. Dalfovo, Phys. Rev. A **71**, R061602 (2005); I. Carusotto, R. Balbinot, A. Fabbri, and A. Recati, Eur. Phys. J. D **56**, 391 (2010).

[34] In the configurations shown in Fig. 6, only the case $\alpha = \pi/2$ is realized. To obtain $\alpha = 0$ with the first choice of level scheme, one may, e.g., choose a sublevel $|b\rangle = |F = 2, m_F = -1\rangle$ and take the coupling beam propagating along x with a linear polarization along y.

[35] The apparent agreement of this value, $f_n \simeq 0.22$, obtained from a quantum Bogoliubov calculation with the result of the classical field simulation of Fig. 3 for $T/T_d = 0.1$, is accidental. A Bogoliubov calculation for the classical field would give a 40% deviation from this value.

[36] Above the critical temperature, there is no superfluid phononic branch, and one may expect that the condition $q\xi \lesssim 1$ for f_n^{eff} to reach the zero-q limit is replaced by the condition that $q\lambda \lesssim 1$, where λ is the thermal de Broglie wavelength, which is less stringent in the high-temperature limit. To test this intuitive idea, Bogoliubov theory is not applicable, but it is tempting to use the ideal gas model as a first guess. For $q\lambda \lesssim 1$ and $T \ll T_d$, one then obtains for the ideal quantum gas in the thermodynamic limit

$$\lim_{\gamma \to 0} \left(f_n^{\text{eff}} - f_n \right) \simeq \frac{2T}{T_d} \left[1 - \frac{\text{atanh} X}{X} \right],$$

with $X = \epsilon/(4 + \epsilon^2)^{1/2}$, $\epsilon^2 = \hbar^2 q^2/(2m|\mu|)$, and the chemical potential $\mu \simeq -k_B T \exp(-T_d/T)$. The condition that this is much smaller than f_n, which is here equal to unity, thus, involves not only a condition on $q\lambda$ but also involves a comparison of $\hbar^2 q^2/2m$ to the chemical potential, which is much more stringent for $T \ll T_d$. This could be expected from the fact that, for the occupation numbers of the low-momenta modes, the Bose-Einstein formula reduces to the Lorentzian shape $n_k \simeq k_B T/(|\mu| + \hbar^2 k^2/2m)$, which has a narrow momentum width $\propto |\mu|^{1/2}$. As an example, to have $f_n^{\text{eff}} = 0.9$ for the ideal gas in the zero γ limit, one has to take $q\lambda \simeq 0.48$ for $T/T_d = 0.18$ and $q\lambda \simeq 0.08$ for $T/T_d = 0.1$ (these values of q correspond to $q\xi = 0.64$ and $q\xi = 0.08$ for the interacting gas with $g = 0.1\hbar^2/m$, respectively).

[37] Yu. Kagan, B. V. Svistunov, and G. V. Shlyapnikov, Sov. Phys. JETP **75**, 387 (1992); Yu. Kagan and B. V. Svistunov, Phys. Rev. Lett. **79**, 3331 (1997); N. G. Berloff and B. V. Svistunov, Phys. Rev. A **66**, 013603 (2002); M. J. Davis, S. A. Morgan, and K. Burnett, Phys. Rev. Lett. **87**, 160402 (2001); K. Góral, M. Gajda, K. Rzażewski, Opt. Express **8**, 92 (2001); D. Kadio, M. Gajda and K. Rzażewski, Phys. Rev. A **72**, 013607 (2005); A. Sinatra, Y. Castin, and E. Witkowska, *ibid.* **75**, 033616 (2007); **80**, 033614 (2009).

[38] C. Lobo, A. Sinatra, and Y. Castin, Phys. Rev. Lett. **92**, 020403 (2004); N. G. Parker and C. S. Adams, *ibid.* **95**, 145301 (2005); J. Phys B **39**, 43 (2006).

[39] More precisely, $\ln \zeta = 4G/\pi - 2\ln 2$, G being the Catalan constant $G \simeq 0.91596\ldots$.

[40] The discrete Laplacian Δ admits the plane waves $e^{i\mathbf{k}\cdot\mathbf{r}}$ as eigenmodes on the lattice with the eigenvalue $\hbar^2 k^2/(2m)$. In practice, a fast Fourier transform is used to evaluate the action of the Laplacian on the field Ψ.

[41] E. Mandonnet, Ph.D. thesis, University Paris 6, 2000 [http://tel.archives-ouvertes.fr/tel-00011872/fr/].

[42] A. Sinatra, Y. Castin, and Yun Li, Phys. Rev. A **81**, 053623 (2010); K. Maussang, G. E. Marti, T. Schneider, P. Treutlein, Y. Li, A. Sinatra, R. Long, J. Estève, and J. Reichel, Phys. Rev. Lett. **105**, 080403 (2010).

[43] For the real-time evolution, the kinetic, external potential, and interaction energy terms are treated with the usual splitting technique, with each corresponding evolution operator being diagonal either in position space or in Fourier space. The evolution operator under the gauge potential (21) during the time-step dt involves numerical evaluation of objects of the form

$$\Psi' = e^{-idt[p_y - h(x,y,t)]^2}\Psi,$$

where we can assume without loss of generality that the function $h(x,y,t)$ has a zero spatial mean over y, $\int_0^L dy h(x,y,t) = 0, \forall x, \forall t$. This requires a bit more care as the evolution operator is not diagonal in the real space, in the **k** space, or in any mixed representation (real space along some direction and Fourier-space along the other). In a first stage, we performed a local gauge transform on Ψ of the form

$$U\Psi = e^{-iH(x,y,t)/\hbar}\Psi,$$

with $\partial_y H(x,y,t) = h(x,y,t)$. In this way, the operator that one has to exponentiate to obtain the evolution operator is simply proportional to p_y^2. Since $h(x,y,t)$ has a zero spatial mean along the y axis, $H(x,0,t) = H(x,L,t), \forall x, \forall t$, so the gauge transform is compatible with the periodic boundary conditions. In a second stage, we realized, however, that this gauge transform trick is not exact for our lattice model, since p_y is not simply $(\hbar/i)\partial_y$ (contrarily to continuous space). As a consequence, relation (E1) was not well satisfied numerically. Since the non-zero-spatial-mean version of $h(x,y,t)$ is factorized in a function $f(x,t)$ of x and t times $\exp[-y^2/(2\sigma^2)]$, with $w = 2\sigma$, we simply diagonalized numerically once the operator $W = p_y \exp[-y^2/(2\sigma^2)] + \text{H.c.}$ (in practice, a 64×64 Hermitian matrix for Fig. 4) and evaluated the evolution operator $\exp[idt f(x,t)W]$ in the corresponding eigenbasis (where it is diagonal).

[44] A. J. Leggett, Rev. Mod. Phys. **71**, S318 (1999).

[45] I. Carusotto and Y. Castin, C. R. Phys. **5**, 107 (2004).

[46] N. Prokof'ev, O. Ruebenacker, and B. Svistunov, Phys. Rev. Lett. **87**, 270402 (2001).

[47] Measuring the gas energy is, in general, reduced to measuring the gas spatial density profile before time of flight (to measure the trapping energy) and after time of flight (to measure the initial kinetic plus interaction energy, which is the expansion energy). These density measurements have reached a precision giving the absolute equation of state of the gas, the pressure for example, within 5% [20,21] or even at the percentage-point level [22] but not yet at the sub-percentage-point level. Our scheme, however, requires a measurement of an energy change, not an absolute measurement of the energy, giving hope for a better precision. Recent experiments have actually measured the change of the momentum [23] and of the energy [24] of a gas to determine its structure factor with good precision, not for a gauge-field excitation as proposed here, but for a Bragg laser excitation.

[48] To avoid the rapid increase of the error bars on f_n for $\epsilon_{\text{gauge}} \to 0$, due to the effect discussed in Appendix E, we performed, for each stochastic field realization of the thermal ensemble, two independent temporal evolutions, one in the presence of the gauge field, **A**, and the other in the presence of the opposite gauge field, $-\mathbf{A}$. We then took the average of the two corresponding deposited energies. This in particular exactly eliminates all the noisy terms in the deposited energy that are linear in the gauge field.

[49] We have checked by performing simulations [for $q\xi = 1$, $\gamma/(c_s q) = 0.4$ and $\epsilon_{\text{gauge}}/(mk_B T_d)^{1/2} = 0.02$] with a duration $\tau = 6/\gamma$ that the truncation of the time evolution at $\tau = 3/\gamma$ as done in Fig. 4 introduces an error on the normal fraction which is within the statistical error bars.

[50] M. Fleischhauer, A. Imamoglu, and J. P. Marangos, Rev. Mod. Phys. **77**, 633 (2005).

[51] L. V. Hau, S. E. Harris, Z. Dutton, and C. H. Behroozi, Nature (London) **397**, 594 (1999).

[52] S. Inouye, R. F. Löw, S. Gupta, T. Pfau, A. Görlitz, T. L. Gustavson, D. E. Pritchard, and W. Ketterle, Phys. Rev. Lett. **85**, 4225 (2000).

[53] P. Öhberg, Phys. Rev. A **66**, 021603 (2002).

[54] M. Artoni and I. Carusotto, Phys. Rev. A **67**, 011602 (2003).

[55] F. Brennecke, S. Ritter, T. Donner, and T. Esslinger, Science **322**, 235 (2008).

[56] Equations (54), (55), (57), (59), and (61) have been obtained from the operatorial form of Eq. (49), where the atomic field operators have already been reduced to 2D. This is an approximation. The exact mean intensity of the light field involves the expectation value of products of $\hat{\phi}_{3D}$ and $\hat{\phi}_{3D}^\dagger$ that are not normally ordered, and one has to put the atomic field operators in normal order before the 2D reduction. In the operatorial form of Eq. (49), this amounts to replacing $\mathbf{k}_c \cdot [\mathbf{j} + \frac{\hbar}{2im}\nabla n]$ with $(\mathbf{k}_c - \mathbf{k}_p) \cdot \mathbf{J}$, where $\mathbf{J}(x,y) = \int_{-\infty}^{+\infty} dz \frac{\hbar}{im}\hat{\phi}_{3D}^\dagger(x,y,z)\nabla\hat{\phi}_{3D}(x,y,z)$. One then finds additive corrections to the above-mentioned equations. For example, for $k_p \simeq k_c$, in Eq. (59) one has to add to the expression $\frac{k_B T \rho(\mathbf{r}_0)}{m}[\cos^2\phi_{\text{sc}} + f_n \sin^2\phi_{\text{sc}}]$ the correction $\hbar\omega_z\rho(\mathbf{r}_0)/(2m)$. This correction, corresponding to spontaneous emission due to the motional coupling between $|\text{NC}\rangle$ and $|C\rangle$ along z, is a flat function of ϕ_{sc} that can thus be distinguished experimentally from the relevant $f_n \sin^2\phi_{\text{sc}}$ component.

[57] As a consequence of the continuity equation, the fluctuations of the density and of the longitudinal current are related by $\omega n_{\mathbf{q}} = \mathbf{q} \cdot \mathbf{j}_{\mathbf{q}}$. For small wave vectors, fluctuations are mostly soundlike with $\omega \simeq c_s q$. Inserting this result into the continuity equation, one finds that $\hbar q n_{\mathbf{q}}/2m \ll j_{L,\mathbf{q}}$ if $q\xi/2 \ll 1$.

[58] M. R. Matthews, D. S. Hall, D. S. Jin, J. R. Ensher, C. E. Wieman, E. A. Cornell, F. Dalfovo, C. Minniti, and S. Stringari, Phys. Rev. Lett. **81**, 243 (1998).

[59] D. S. Hall, M. R. Matthews, J. R. Ensher, C. E. Wieman, and E. A. Cornell, Phys. Rev. Lett. **81**, 1539 (1998); D. S. Hall, M. R. Matthews, C. E. Wieman, and E. A. Cornell, *ibid.* **81**, 1543 (1998).

[60] J. M. Vogels, C. C. Tsai, R. S. Freeland, S. J. J. M. F. Kokkelmans, B. J. Verhaar, and D. J. Heinzen, Phys. Rev. A **56**, R1067 (1997).

[61] For a review on atomic collisions, see, e.g., C. Chin, R. Grimm, P. Julienne, and E. Tiesinga, Rev. Mod. Phys. **82**, 1225 (2010) and references therein.

[62] A. Robert, O. Sirjean, A. Browaeys, J. Poupard, S. Nowak, D. Boiron, C. I. Westbrook, and A. Aspect, Science **292**, 461 (2001).

[63] F. Pereira Dos Santos, J. Léonard, Junmin Wang, C. J. Barrelet, F. Perales, E. Rasel, C. S. Unnikrishnan, M. Leduc, and C. Cohen-Tannoudji, Phys. Rev. Lett. **86**, 3459 (2001).

[64] J. Dalibard, F. Gerbier, G. Juzeliunas, P. Öhberg, e-print arXiv:1008.5378.

[65] Note that, for the second choice of laser configuration to come, atoms with a $J = 1 \to J' = 1$ transition and a large fine structure are quite favorable, because the spurious light shift

U^p is strongly suppressed. Also, since $|a\rangle = |J = 1, m = -1\rangle$ and $|b\rangle = |J = 1, m = 0\rangle$, one finds $g_{aa} = g_{ab}$ from rotational symmetry arguments [66,67]. A potential problem to take care of is the partial inelastic nature of the *b*-*b* collisions.

[66] T. L. Ho, Phys. Rev. Lett. **81**, 742 (1998); W. Zhang and D. F. Walls, Phys. Rev. A **57**, 1248 (1998); T. Ohmi and K. Machida, J. Phys. Soc. Jpn. **67**, 1822 (1998).

[67] Y. Castin and C. Herzog, Comptes Rendus de l'Académie des Sciences de Paris, tome 2, série IV, (Elsevier, Paris, 2001), p. 419.

[68] This choice for $|e\rangle$ increases the branching ratio B of Eq. (51) by a factor of 3 with respect to the choice $|F' = 1, m_{F'} = -1\rangle$.

[69] We have checked that the contribution to $\langle C| - \partial_t |NC\rangle$ of the switch-off function $f(t)$ in Ω_p [that was not included in Eq. (45)] gives a negligible correction to the estimate of the fluorescence rate.

[70] Any two-photon Raman coupling of the $|NC\rangle$ state to $|c\rangle$ via the excited state sublevel $|e\rangle$ vanishes thanks to the destructive interference of the two paths $|a\rangle \rightarrow |e\rangle \rightarrow |c\rangle$ and $|b\rangle \rightarrow |e\rangle \rightarrow |c\rangle$.

[71] F. Gerbier and Y. Castin, Phys. Rev. A **82**, 013615 (2010).

[72] At the lowest order in Ω_p/Ω_c, the effect of a nonzero $g_{aa} - g_{ab}$ for the measurement scheme of Sec. V A is to introduce a smooth polarization profile $\mathcal{P}_p = [4|d_{ae}|^2/(\hbar^2|\Omega_c|^2)](g_{aa} - g_{ab})\langle\phi_{3D}^{\dagger 2}\phi_{3D}^2\rangle\mathcal{E}_p$. As the corresponding phase shift does not depend on Ω_p/Ω_c, it can be isolated in the experiment. The contribution of higher-order terms $O(|\Omega_p/\Omega_c|^3)$ have a nontrivial spatial structure and may interfere with the signal to be measured. Their relative value as compared to $\Delta\phi_2$ is, however, a factor roughly $[(g_{aa} - g_{ab})/g_{aa}]\tilde{g}(\rho\lambda_c^2)/(2\pi^2 f_n)$ weaker.

[73] We have checked that the right-hand side of Eq. (C13) is simply $-\Delta F$ (within linear response theory), where ΔF is the free energy of the system at thermal equilibrium in presence of the static gauge field $\mathbf{A}(\mathbf{r}, 0^+)$ minus the free energy in the absence of gauge field for fixed temperature and atom number. This establishes a formal link between our proposal and the one of Ref. [9].

[74] We used the fact that, for a generic function F satisfying $F[-(\mathbf{k} + \mathbf{q})] = F(\mathbf{k})$ for all $\mathbf{k}$, one has $\sum_{\mathbf{k}\neq\mathbf{0}, -\mathbf{q}:k_y>0} F(\mathbf{k}) = \sum_{\mathbf{k}\neq\mathbf{0}, -\mathbf{q}:k_y<0} F(\mathbf{k})$.

[75] M. Greiner, C. A. Regal, J. T. Stewart, and D. S. Jin, Phys. Rev. Lett. **94**, 110401 (2005); S. Fölling, F. Gerbier, A. Widera, O. Mandel, T. Gericke, and I. Bloch, Nature **434**, 481 (2005); T. Rom, Th. Best, D. van Oosten, U. Schneider, S. Fölling, B. Paredes, and I. Bloch, *ibid.* **444**, 733 (2006); A. Perrin, H. Chang, V. Krachmalnicoff, M. Schellekens, D. Boiron, A. Aspect, and C. I. Westbrook, Phys. Rev. Lett. **99**, 150405 (2007); T. Jeltes *et al.*, Nature **445**, 402 (2007); S. Hofferberth, I. Lesanovsky, T. Schumm, A. Imambekov, V. Gritsev, E. Demler, and J. Schmiedmayer, Nat. Phys. **4**, 489 (2008).

[76] E. Altman, E. Demler, and M. D. Lukin, Phys. Rev. A **70**, 013603 (2004); I. Carusotto and Y. Castin, Phys. Rev. Lett. **94**, 223202 (2005); V. Gritsev, E. Altman, E. Demler, and A. Polkovnikov, Nat. Phys. **2**, 705 (2006); I. Carusotto, S. Fagnocchi, A. Recati, R. Balbinot, and A. Fabbri, New J. Phys. **10**, 103001 (2008).

[77] L. P. Pitaevskii and S. Stringari, *Bose-Einstein Condensation* (Clarendon Press, Oxford, 2003).

[78] A sufficient condition is that the uncertainty in the initial total energy is $\ll \hbar\gamma$.